Filipe Miguel Ramos da Cruz Soares

Degree in Environmental Engineering Sciences

Development of tools for the management of oyster nurseries: static and dynamic modelling

Dissertation submitted to obtain the degree of Master in Environmental Management Systems

Supervisor: Ana Maria Nobre, Postdoctoral Researcher, CIIMAR
Co-supervisor: João Gomes Ferreira, Tenured Associate Professor with *Agregação*, FCT-UNL

Jury:

President: Prof. Maria Helena Costa
Examiner: Prof. Paulo Alexandre Diogo
Examiner: Dra. Ana Maria Nobre

FACULDADE DE CIÊNCIAS E TECNOLOGIA
UNIVERSIDADE NOVA DE LISBOA

November 2017

Filipe Miguel Ramos da Cruz Soares

Degree in Environmental Engineering Sciences

Development of tools for the management of oyster nurseries: static and dynamic modelling

Dissertation submitted to obtain the degree of Master in Environmental Management Systems

Supervisor: Ana Maria Nobre, Postdoctoral Researcher, CIIMAR
Co-supervisor: João Gomes Ferreira, Tenured Associate Professor with *Agregação*, FCT-UNL

Jury:

President: Prof. Maria Helena Costa
Examiner: Prof. Paulo Alexandre Diogo
Examiner: Dra. Ana Maria Nobre

FACULDADE DE CIÊNCIAS E TECNOLOGIA
UNIVERSIDADE NOVA DE LISBOA

November 2017

Development of tools for the management of oyster nurseries: static and dynamic modelling

Acknowledgments

First of all, I would like to thank my supervisor, Ana Nobre, for the opportunity, guidance, support, and for all the trust placed in me. It was a pleasure to work with her, in which I learned a lot. I'm really grateful.

In second, I would like to thank my co-supervisor and professor, João G. Ferreira, the availability and helpful comments during this work. I cannot fail to mention all the guidance, and awareness for certain themes, provided during my years of study. It was very inspiring to me.

I would like to thank Rui Moreira and François Hubert, from Bivalvia, for the opportunity to develop the case study for Bivalvia's nursery, as well as their availability to provide me all the necessary knowledge and data about the system.

To Richard Langton, for the kindness to provide me some additional information about the experimental conditions of one of his published experiments.

To Joana, for the helpful review of the grammatical construction of writing.

To Julia, for all the patience, support, discussions, and funny moments, which help me a lot during this work.

In last, but not least, I would like to thank all my family and friends. Special thanks to my dad, for investing in my education and always supporting me in everything.

Abstract

Ecological models have been applied for carrying capacity assessments of oyster aquaculture, and have shown to be very useful in guiding the planning and management towards production optimization. However, the existing models are mostly directed to the grow-out phase (production of adult oyster), lacking models to be applied in nurseries (production of juvenile oyster).

This work presents two models to support the management of oyster nurseries that are targeted to farmers:

- A static mass balance model for oyster nurseries, which estimates the maximum stock for typical external food concentrations of the nursery. Part of the work developed herein contributed to its development (available online at: http://seaplusplus4.com/oysterspatbud.html).
- A dynamic model for oyster nurseries, which simulates the individual growth, food availability and stock evolution over time. The model was conceptualized and implemented as part of this work, and further validated with three data sets from the scientific literature.

In this work, it is shown the application of both models to simulate a commercial nursery. The results show that both models can provide useful information, and thus guidance to farmers, even when there is a lack of data or knowledge about some features of the system, required to properly drive the models.

Key-words: Pacific oyster, *Crassostrea gigas*, Spat, Nursery, Carrying capacity, Mass balance model, Dynamic model.

Resumo

Modelos ecológicos têm sido aplicados para a avaliação da capacidade de carga da aquacultura de ostra, demonstrando serem muito úteis na orientação do planeamento e gestão em direção à otimização da produção. No entanto, os modelos existentes são na sua maioria direcionados à fase de engorda (produção de ostra adulta), faltando modelos para serem aplicados em berçários (produção de ostra juvenil).

Este trabalho apresenta dois modelos para apoiar a gestão de viveiros de ostra, e direcionam-se aos produtores:

- Um modelo estático de balanço de massas para viveiros de ostra, o qual para típicas concentrações de alimento no exterior do berçário estima o máximo estoque a sustentar. Parte do trabalho desenvolvido aqui contribuiu para o seu desenvolvimento (disponível online em: http://seaplusplus4.com/oysterspatbud.html).
- Um modelo dinâmico para viveiros de ostra, que simula o crescimento individual, a disponibilidade de alimento e a evolução do estoque ao longo do tempo. O modelo foi conceptualizado e implementado como parte deste trabalho, e validado para três conjuntos de dados da literatura científica.

Neste trabalho, mostra-se a aplicação de ambos os modelos para simular um viveiro comercial. Os resultados mostram que ambos os modelos podem fornecer informações úteis e, portanto, orientações aos produtores, mesmo quando há falta de dados ou conhecimento sobre algumas características do sistema, necessários para correr adequadamente os modelos.

Palavras-chave: Ostra do Pacífico, *Crassostrea gigas*, Spat, Berçário, Capacidade de carga, Modelo de balanço de massas, Modelo dinâmico.

Table of Contents

List of Figures

List of Tables

List of Abbreviations

ADCP – Acoustic Doppler Current Profiler

Chl-*a* – Chlorophyll-*a*

DEB – Dynamic Energy Budget

DW – Tissue Dry Weight

FAO – Food and Agricultural Organization of the United Nations

FLUPSY – Floating Upwelling System

IMTA – Integrated Multi-Trophic Aquaculture

NEB – Net Energy Balance

NOAA – National Oceanic and Atmospheric Administration

NS – North System

POC – Particulate Organic Carbon

POM – Particulate Organic Matter

SFG – Scope For Growth

SMR – Standard Metabolic Rate

SS – South System

TFW – Total Fresh Weight

USA – United States of America

1. Introduction

Aquaculture was responsible for 53% of the global seafood production (in quantity) in 2015 (FAO, 2017a). At global level stands as the fastest growing food sector, with production increasing at an average of about 6% per annum since the start of the millennium (FAO, 2017a). Prospects point that in the future aquaculture will play an increasingly important role in the supply of seafood (Msangi et al., 2013; Kobayashi et al., 2015). On the one hand world's human population is increasing fast (FAO, 2017b; Samir & Lutz, 2017), which means a higher demand for food in the future, on the other hand the marine biodiversity is being threatened by overfishing, pollution and habitat destruction (Lotze et al., 2006; Halpern et al., 2007; Zhou et al., 2015), which can lead to a crisis in global fisheries by mid-century (Worm et al., 2006; Pauly & Zeller, 2017). Bringing new solutions to the aquaculture sector, aiming a sustainable improvement of its production potential, is a key-point to maintain the growth of the sector.

One important share of this sector is the bivalve production. Latest data from FAO (2017), relative to 2015, point that bivalve production accounts for 14% of global aquaculture production (in quantity), of which oysters represent 36%. Aquaculture stands as the main source of oyster production (~97%), being the Asian continent the larger contributor with around 95% of the global farmed volume, followed by the American and European continents (around 3% and 2%, respectively). The Pacific Oyster (*Crassostrea gigas*, Thunberg) stands out as the most significant species from all the world's oyster production (FAO, 2017a). It presents a considerable economic value and it is seen as an attractive species by farmers due to its rapid growth in comparison with other oyster species (Ruesink et al., 2005).

Oyster production in aquaculture typically involves three stages: (i) hatchery, specialized in the development of early stages of these organisms (i.e. larvae and small spat), occurring these operations generally in land-based farms; (ii) nursery, focused on rearing oyster spat (seeds) until reaching a sufficient size to be planted in the field, with operations occurring in closed or open upwelling systems (e.g. FLUPSY); and (iii) grow-out, the oyster farming in the field (e.g. estuaries) until they reach the harvestable size to be commercialized, whereby several farming methods can be used, including on-bottom and off-bottom cultures (Flimlin, 2000; Helm & Bourne, 2004; Doiron, 2008).

The filter-feeding behavior of oysters is considered an important feature of oyster farming, with multiple implications at functional, operational, and environmental level. Oysters feed on microalgae and other organic matter suspended in the water column (Bayne, 2017). Most of its

production cycle rely on the availability of food in the surrounding environment, with exceptions for hatchery operations where the early stages of this organisms are fed with cultured microalgae (Helm & Bourne, 2004). As oysters do not need external feed inputs, like other non-fed cultures (e.g. seaweeds, carps, and other filter-feeding shellfish), their production is seen as attractive. Furthermore, oyster farming can be included in an integrated multi-trophic aquaculture (IMTA), in which organic waste from other adjacent fed aquacultures (e.g. of finfish) can contribute as an additional source of food, thus enhancing the oyster growth or the production capacity, while the oysters, on the other hand, can act as reducers of the environmental impact of organic waste from fish-farming activities (see e.g. Ferreira et al., 2012; Jiang et al., 2013). Other potential ecosystem and ecological benefits, provided by oyster farming, are nowadays widely recognized, including nutrient cycling, top-down control of primary symptoms of eutrophication, benthic-pelagic coupling, refuge from predators, and among others (Dumbauld et al., 2009; Forrest et al., 2009; Higgins et al., 2011). Of relevant importance for farmers are the processes of nutrient cycling and the benthic-pelagic coupling, which may in some cases be translated into an opportunity for additional profit, either by the potential of farmers to benefit, in the near future, from nutrient credit trading programs (Jones et al., 2010; Newell & Mann, 2012; Filgueira et al., 2015a; Ferreira & Bricker, 2016), or by the potential of inclusion of other cultures, in an IMTA, to reuse the deposited organic waste of oyster farms (see e.g. Paltzat et al., 2008).

Despite the previously described benefits, oyster farming, as well as other bivalve sectors, may also have environmental, ecological and social impacts (Kaiser et al., 1998; Crawford et al., 2003; Forrest et al., 2009). One of the main concerns of bivalve farming is the assessment of its sustainability. Linked to this concern is the concept of carrying capacity, that describes the relationships between the size of the production and the change of resources on which it depends (see review of McKindsey et al., 2006). Inglis et al., (2000) defines four types of carrying capacity: physical, production, ecological and social. Applications of this concept are based on well-defined objectives, which implies the definition of the scale and its interactions. Usually, these assessments are carried out at the system scale (bay, estuary or related sub-units), or at the local scale (farm). As the oyster farming generally relies on the rates by which food is renewed in the surrounding environment, which is a function of primary production and water residence time, one relevant issue to the farmers is to know if this availability can sustain a given production, aiming towards the maximization of harvests. Therefore, the assessment of the production carrying capacity, defined by Inglis et al., (2000) as “the stocking density of bivalves at which harvests are maximized”, it is of important matter for the stock management.

Ecological models have proven to be useful in this assessment (see e.g. Duarte et al., 2003; Nunes et al., 2003; Grant et al., 2007; Ferreira et al., 2007; Guyondet et al., 2010), thus becoming powerful tools to be used by shellfish farmers or consultants related with this sector. Models developed in this scope usually incorporate a different set of sub-models, as: (i) a hydrodynamic model, which simulates the motion, transportation and transfer of particles or substances (e.g. food and nutrients); (ii) a primary production model, that simulates the primary production within the considered system; and (iii) a bioenergetic model, which simulates the energy allocation in a certain bivalve species under different food and environmental conditions. Some of this models include other components (e.g. ecological and economic), and couple the bioenergetics modelling of more than one species (Nunes et al., 2003; Ferreira et al., 2007).

Bioenergetic models of bivalves are constructed based on mathematical functions that represent the physiological processes of an organism, which requires a broader knowledge of its physiology. In the majority of the cases, this functions derive from laboratory experimental data, depending its formulation on the conditions of the experiments, e.g. temperature, salinity, suspended matter quality and quantity, among others (e.g. Bayne, 1999; Ren et al., 2000). The conceptualization of this models is based on theories of energy allocation. Traditional bioenergetics theories, e.g. net energy balance (NEB) or scope for growth (SFG), describe energy acquisition from feeding and its partitioning among processes as respiration, activity, reproduction, excretion and growth (Winberg, 1960), whilst the energy budget (DEB) theory (Kooijman, 2000) describes the individual in terms of structural body and reserves, being that the energy acquired from feeding is allocated to the reserves before being used for somatic maintenance, growth, maturity maintenance, maturation and reproduction (van der Meer, 2006).

Due to the commercial importance of *Crassostrea gigas,* a vast set of bioenergetic models have been developed regarding this species. Some are based on the NEB or SFG approach (Barillé et al., 1997; Kobayashi et al., 1997; Hyun et al., 2001; Méléder et al., 2001; Hawkins et al., 2013) and others on the DEB approach (Ren & Ross, 2001; Bacher & Gangnery, 2006; Pouvreau et al., 2006; Ren & Schiel, 2008; Bourlés et al., 2009; Grangeré et al., 2009; Alunno-Bruscia et al., 2011). Most of these models are for adult oysters and some may also include the simulation of oyster spat (juveniles). However, the inclusion of oyster spat is done by adapting some functions, which define physiologic processes, to better represent the oyster spat behavior. Because oysters spat have high variable physiologic rates over its size spectrum, these adaptations become insufficient. Therefore, the development of models only focused on oyster spat may be a way to better model this variability.

Given that oyster nurseries are commonly extensive systems, as they hinge on the food available in the surrounding environment, and in some cases from phytoplankton blooming ponds (used to induce phytoplankton growth), ecological models may play an important role in the nursery management and sustainability assessments (e.g. models to assess the production carrying capacity). However, models of this type, applicable in oyster nurseries, are lacking from the scientific literature.

1.1. Objectives

The work developed herein intends to fill the lack of ecological models applicable to oyster nurseries, aiming:

- A simplified simulation of the oyster nursery to assess the maximum stock sustained, by means of a static model.
- A dynamic simulation of oyster spat individual growth, food availability within the farming system and stock biomass, by means of a dynamic model.

It is expected that these models can be used as tools for the management of oyster nurseries, by providing knowledge about the system behavior under different conditions.

The overall objective of this work is the application of both models in a commercial nursery, aiming at guide the management for production optimization.

2. General approach

2.1. Overview

Taking into account that the level of knowledge about the system conditions may differ among oyster nurseries managers, it was followed two modelling approaches: (i) a static and simplified, which requires a lower level of input data, but which in turn provides limited output data; and (ii) a dynamic, which requires a higher level of input data, thus providing a wider range of output data. Despite the differences, both approaches have the common objective of guiding the management for production optimization.

For an overall assessment of the maximum stock for typical external food concentrations at the nursery a static mass balance model for oyster nurseries was used (Section 3, available online at: http://seaplusplus4.com/oysterspatbud.html). This model resulted from a collaborative work, in which part of it was developed within the scope of this thesis. The final work was consolidated into a research paper (presented in Section 3), which was accepted for publication by the Journal of Shellfish Research.

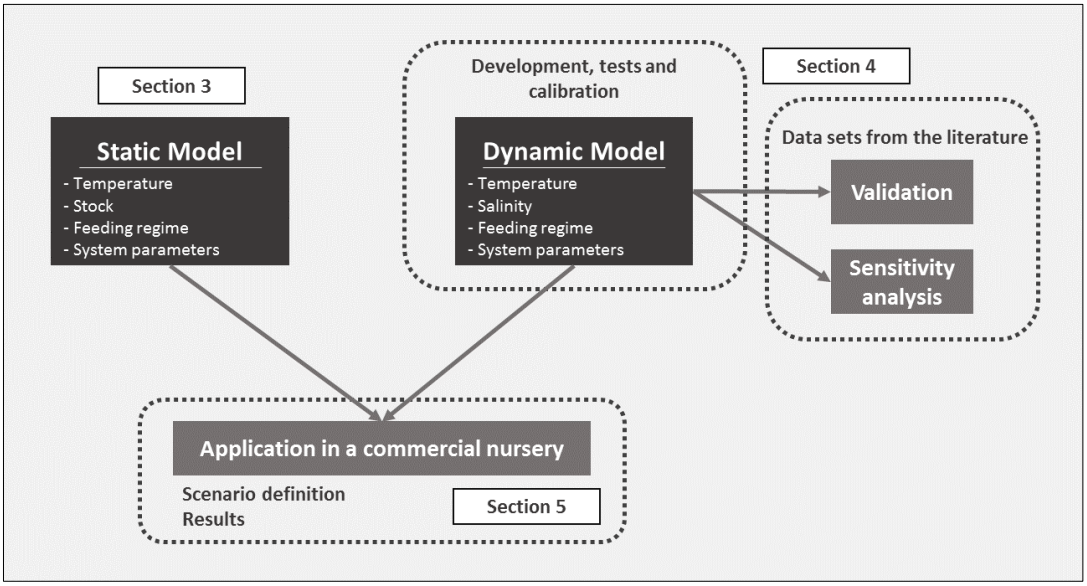

Figure 2.1 - Thesis Framework.

For the simulation of oyster spat individual growth, food availability within the farming system and stock biomass over time, a dynamic model for oyster nurseries was developed (Section 4). This model couples a single compartment mass balance model with an individual bioenergetic model of *Crassostrea gigas* spat, both constructed based on knowledge and data from the scientific literature. A web-based simulation and modelling tool, Insight Maker (Fortmann-Roe, 2014), was used to implement it. The model was validated for datasets from the scientific literature and a sensitivity analysis was carried out to assess the model's robustness.

Both models were applied in a commercial nursery, operated by Bivalvia – Mariscos da Formosa, Lda (Section 5). Hypothetical scenarios were defined and guided by the farm operational manager and aimed at the identification of key-factors for production optimization.

2.2. Case study – Bivalvia's commercial nursery

Bivalvia's nursery is located within the Ria Formosa (37°00'58.6"N and 7°52'55.8"W, Figure 2.2), a complex inshore coastal system located in southern Portugal, with the status of marine protected area. With an extent of 55 km (W-E) and 6 km (N-S), the Ria Formosa is separated from the sea by sandbanks and several barrier islands. The tidal range is between 0.9 and 3.0 m (Ferreira et al., 2014), being considered as mesotidal. About 50 to 75% of its water volume is renewed daily due to the tides (Newton & Mudge, 2003), becoming the large mudflats exposed at low tide and submerged at high tide (Neves, 1988).

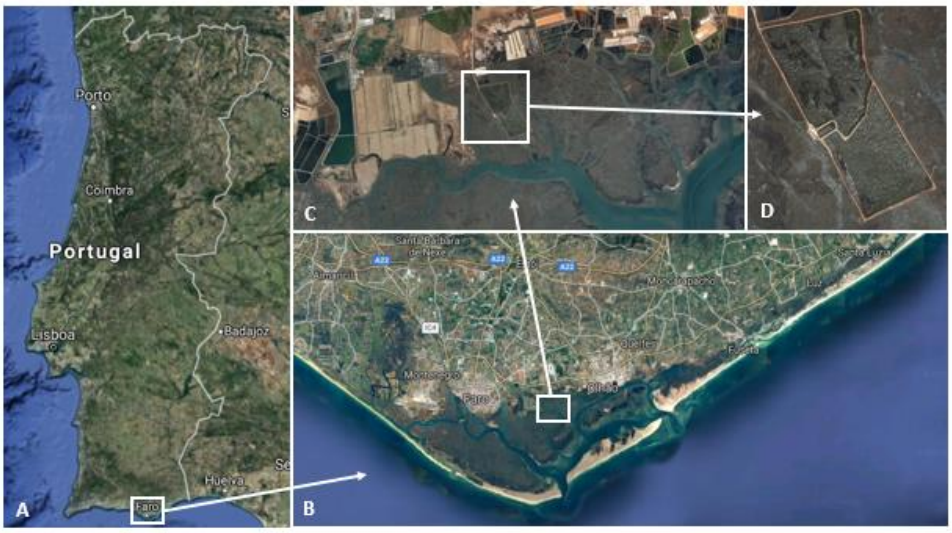

Figure 2.2 - Commercial nursery location: A) Portugal; B) Ria Formosa; C) and D) – Satellite view of the commercial nursery.

At the national level the Ria Formosa stands as the most productive aquaculture zone, being simultaneously the home of multiple socio-economic activities such as tourism, salt extraction, fisheries, effluent discharges, among others (Ceia et al., 2010; Ferreira et al., 2013; Ferreira et al., 2014).

Inserted in earth ponds, Bivalvia's nursery is composed by one rearing tank, which incorporates a floating upwelling system (FLUPSY), and two adjacent blooming ponds, that promote the natural growth of phytoplankton (NS – north system, and SS – south system), being operated as an extensive system (i.e. without the supply of artificial food or nutrients).

The FLUPSY (Figure 2.3) is a shellfish nursery system designed to increase the water flow efficiency, and therefore the rate at which the food is delivered to the post-settled shellfish. Usually, this type of systems are placed in productive coastal waters and are incorporated into a floating dock (Meseck et al., 2012).

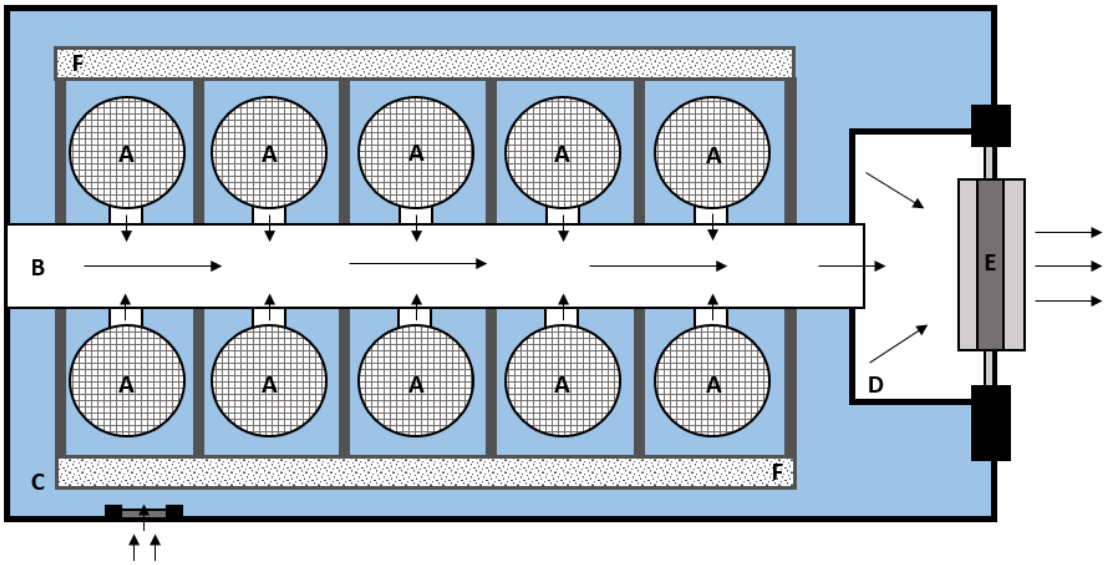

Figure 2.3 - Scheme of the commercial nursery FLUPSY (top view), where the arrows represent the direction of the water flow and: A) Oyster silos with mesh bottom; B) Central water channel; C) Rearing tank; D) Intermediate tank; E) Propeller; F) Floaters.

In the commercial nursery, the oyster spat are placed inside silos with mesh bottoms (A), divided by size classes (Table 2.1), where an upwelling current flows through it. The silos are connected to a central water channel (B), which in turn is connected to an intermediate tank (D). An electric propeller (E), installed on the boundary that separates the intermediate tank from the phytoplankton blooming ponds, induce the current by expelling the water to the phytoplankton blooming ponds.

Table 2.1 - Biomass and mean individual weight of the commercial nursery oyster size class.

Oyster size class	Biomass (g TFW)	Mean individual weight (g TFW)
T3	0.03 – 0.05	0.04
T4	0.05 – 0.125	0.0875
T6	0.125 – 0.25	0.1875
T8	0.25 – 0.8	0.525
T10	0.8 – 1.6	1.2
T12	1.6 – 2.8	2.2
T15	2.8 – 5.5	4.15
T20	5.5 – 10	7.75

The commercial nursery operates with just one phytoplankton blooming pond connected to the FLUPSY, while the other remains without use to accumulate phytoplankton biomass. The daily water renewal is about 2 to 5% of the production tank volume. Each phytoplankton blooming pond has an approximate area of 70 000 and 54 000 m^2 (NS and SS respectively) with an average depth of 1 m. The rearing tank has an area of about 1 000 m^2 with an average depth of 1.3 m. Considering a total water mix in each blooming pond, i.e. without "dead zones", it is assumed a overall system volume of 71 300 m^3 when NS is operating, and a volume of 55 300 m^3 for the case of SS being in operation.

Along the year water salinity remains at 36 psu, with minor fluctuations, and the water temperature ranges between 15 and 29˚C (Figure 2.4, François Hubert, Bivalvia, personal communication). Historic water samples indicate a phytoplankton concentration inside the production tank up to about 200 cells μL^{-1}, and a phytoplankton concentration in the external water channel ranging between 0.3 – 1.0 cells μL^{-1} (François Hubert, Bivalvia, personal communication). These water samples were only carried out for some months, for short intervals, and done with the production system working, not allowing a good representation of the system conditions during all the year as well as an accurate initial tank concentration.

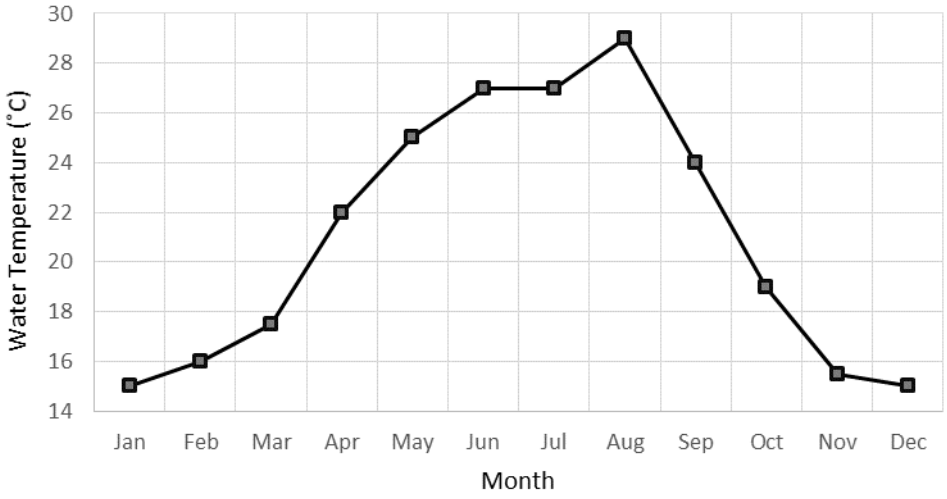

Figure 2.4 - Mean monthly water temperature in the commercial nursery.

3. A static mass balance model for oyster nurseries

This section presents a static mass balance model, which can be used to assess the feeding requirements of a given stock or the maximum stocks sustained for a given feeding regime within an oyster nursery.

This model resulted from a collaborative work, in which a part of it was developed within the scope of this thesis, namely the definition of clearance rates and conversion factors, as well as the acquisition of datasets for model validation. The collaborative work was consolidated into a research paper which was accepted for publication by the Journal of Shellfish Research. The accepted version of the full manuscript is herein included, whereby the *Introduction* puts in context specific aspects of the development of the simple mass balance model.

This section corresponds to a manuscript currently accepted for publication to the Journal of Shellfish Research:

A mass balance model to assess food limitation in commercial oyster nurseries, by Nobre, A.M; Soares, F.; Ferreira, J.G.

A mass balance model to assess food limitation in commercial oyster nurseries

ABSTRACT

This work presents a modelling application designed to provide practical guidance about food limitation in oyster nurseries for seed stock management. The model was implemented and evaluated for the Pacific oyster (*Crassostrea gigas* Thunberg). Scientific knowledge about feeding activity of oyster spat was embedded into a single compartment mass balance. This approach applies to enclosed nurseries such as floating upwelling systems (FLUPSY) or land-based tanks. The mass balance model estimates the i) optimal stock as a function of typical external food concentrations, or ii) the food concentration required for a given stock.

Overall this work aims to support oyster farming which is an important activity from a socio-economic standpoint and for the provision of ecosystem services. While existing ecological models are widely applied for understanding the interactions between the wider ecosystem and farming systems, models are seldom targeted and used directly by farmers. Oyster farmers can use the model to improve the application of general rules of thumb to estimate the stock biomass to hold in their nursery. The mass balance model presented herein is available online (http://seaplusplus4.com/oysterspatbud.html) for widespread use.

INTRODUCTION

Bivalve production accounted for 14 % (in volume) of global aquaculture production of all aquatic species in 2015, of which oysters represent 36% (FAO 2017a). Aquaculture is the main source for oyster production worldwide (~97%, FAO 2017a). According to FAO (2017a) dataset s in 2015 Asia contributed around 95% of the global oyster farming volume (corresponding to about 81% in value); the remaining 5% of the oyster aquaculture production is from North and South American and European continents. Oyster farming is generally regarded as a sustainable sector within the aquaculture industry. It is widely recognized that oyster production, among other filter feeders can provide a set of ecosystem and ecological benefits such as nutrient cycling, integrate the extractive component of integrated multitrophic aquaculture (IMTA) systems, reduction of eutrophication symptoms, habitat provision to other marine species and restocking of wild population (Baker et al. 2015, Coen et al. 2011, Depiper et al 2017, Ferreira et al. 2011, Gallardi 2014, Rose et al. 2014). Furthermore, to grow these extractive species shellfish farmers are major stakeholders to promote good water quality to ensure this industry sustainability as illustrated by Dewey et al. (2011). Shellfish farming is promoted and recognized

by some governmental stakeholders as providing social and economic benefits besides the ecological benefits, e.g. NOAA established in 2011 the USA National Shellfish Initiative.

Most oyster farming practices depend on the natural environment, and like many other farmed species their growth and production hinge on a complex interaction of factors such as temperature, salinity, upstream freshwater flow/rainfall, current speed, density, food concentration and type of the phytoplankton community, food partitioning with other species and disease outbreaks. Modelling can be useful for understanding the feedback between the farming and environmental systems and the effects on production. As an example, carrying capacity models are often applied for management and spatial planning of filter feeder production, as reviewed by Byron & Costa-Pierce (2013) and by Filgueira et al. (2015b). Many other model applications exist for integrated management of oysters and other shellfish production including at ecosystem and farm scales (e.g., Cerco & Noel 2007, Ferreira et al. 2011, Filgueira et al. 2015b, Gangnery et al. 2011, Nobre et al. 2011). Farmers are seldom the target end-users of these models. A strategy to make available simulation models that embed scientific research to farmers is to shift from i) complex models (in terms of spatial and temporal resolutions, processes simulated) that allow detailed simulations but require dataset s that might not be feasible to gather by a commercial unit, to ii) simple models or at least with simple interfaces that can be directly used by farmers and provide estimates of key questions for production; e.g. http://www.farmscale.org/ and Nobre et al. (2017).

Within the shellfish models most of the developments are for adult oysters, few models are suited to simulate initial oyster development stages (e.g., Rico-Villa et al. 2010). Given the high filtration and rapid growth rates of bivalve spat, mass balance models help estimate food requirements for a given stock (the initial seeding stock or the expected stock to harvest). Furthermore, spat are commonly reared in extensive nurseries that rely on natural seston concentration to feed the stock or are coupled with natural blooming tanks. For these systems, it is more difficult to provide guidance on seed stock density given that local food concentration is variable in opposition to hatcheries. For hatcheries and nurseries fed with algae cultures there are, for instance, available online manuals of oyster culture that include guidance for feed ration calculation (e.g. Helm & Bourne 2004, Breese & Malouf 1975, Tetrault 2012, Wallace et al. 2008). Guidance for cultivation practice in spat nurseries is provided based on rules of thumb about typical number of seeds per area or stock biomass to hold in each system based on expert knowledge for similar conditions. On the other side of the spectrum is extensive research about effect of body weight, temperature, food concentration, feeding strategy, among other on the filtration rate, assimilation efficiency and growth of bivalves (Bacher & Baud 1992, Bougrier et

al. 1995, Cranford et al. 2011, Gerdes 1983a, Tamayo et al. 2014, Walne 1972, Ward & Shumway 2004, Winter 1978).

Mass balance models can help to translate scientific knowledge into practical guidance for commercial nurseries using simple user interfaces. The goal of this paper is to develop and evaluate this concept using the Pacific oyster (*Crassostrea gigas* Thunberg) spat as a case study for model implementation and evaluation for enclosed systems such as a floating upwelling system (FLUPSY) or land-based tanks, silos, or trays. The objective is to make the model available online for wider usability and it should tackle two questions that arise when planning or managing an oyster nursery: How much food is required to sustain a given stock and/or for a typical range of food available at surrounding environment what is the maximum biomass to stock in the farm. Further work can be developed for model implementation for other relevant species depending on available research literature and farmers interest: eastern oyster (*Crassostrea virginica* Gmelin), European flat oyster (*Ostrea edulis* Linnaeus), Olympia oyster (*Ostrea lurida* Carpenter), Portuguese oyster (*Crassostrea angulata* Lamarck), slipper cupped oyster (*Crassostrea iredalei* Faustino), Sydney rock oyster (*Saccostrea glomerate* Gould).

METHODOLOGY

Conceptual model description

The model developed herein estimates two independent outputs: i) the required food inputs for a given stock biomass and ii) the maximum stock biomass given a typical external food concentration. It consists of a one compartment mass-balance at steady-state (Figure 3.1):

$$MF_{Food\_in} + MF_{Phyto\_Growth} = MF_{Food\_out} + MF_{Food\_Cleared} \quad \text{(Eq. 3.1)}$$

Whereby, i) the compartment represents an oyster nursery, ii) sources include food inflow (MF_{Food_in}, Eq. 3.2) and phytoplankton growth (MF_{Phyto_Growth}, Eq. 3.3), and iii) sinks include food cleared by oysters ($MF_{Food\_Cleared}$, Eq. 3.5) and food outflow (MF_{Food_out}, Eq. 3.4). The model is targeted at extensive farmers that rely on external natural food resources, represented by MF_{Food_in}. It can also be applied to fed systems considering in that term (i.e., MF_{Food_in}) the feed ration. The model also includes phytoplankton growth (MF_{Phyto_Growth}) to accommodate the cases of nurseries with food supplied by phytoplankton blooming ponds (if that is not the case then $MF_{Phyto\_Growth} = 0$).

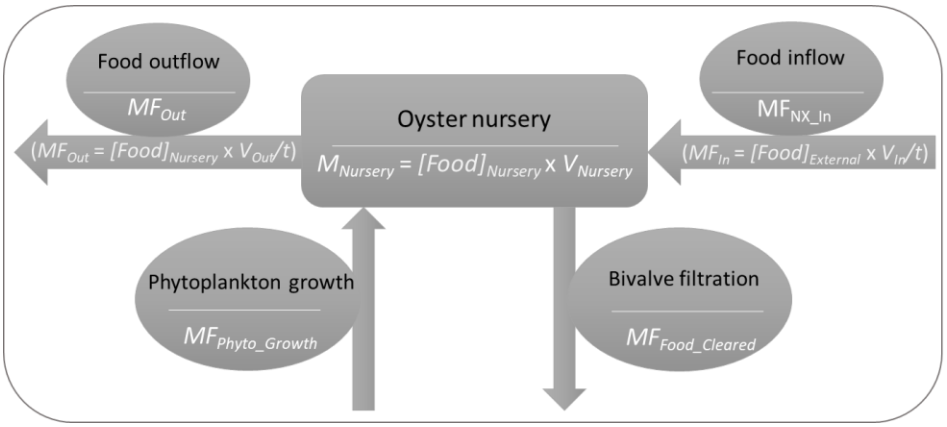

Figure 3.1 - Conceptual model for the oyster nursery.

Oyster food can be expressed using different indicators, such as phytoplankton (or its proxy chl-*a*), particulate organic matter (POM) and particulate organic carbon (POC), among other. To allow model generality food parameters are expressed using several optional oyster food indicators (Table 3.1).

Table 3.1 - Oyster food indicators and corresponding model units.

Oyster food indicator		**Corresponding model units**			
		Food concentration: $[Food]_{External}$ and $[Food]_{nursery}$		**Food fluxes: MF_x**	
Phytoplankton (or a proxy chl-*a*)	Algae biovolume	Per water volume	mm^3 algae.L^{-1}	Per time	mm^3 algae.day^{-1}
	Cell count		algal cells.μL^{-1}		10^6 algal cells.day^{-1}
	Algal mass		mg algae.L^{-1}		mg algae.day^{-1}
	Chl-*a* mass		µg Chl-*a*.L^{-1}		µg Chl-*a*.day^{-1}
POM	Mass		mg POM.L^{-1}		mg POM.day^{-1}
POC	Mass		mg POC.L^{-1}		mg POC.day^{-1}

All mass fluxes (MF_x, Figure 3.1) are expressed in one of the food indicators (defined in Table 3.1) per time and are defined as follows:

MF_{Food_in}, (Eq. 3.2) is given by the external food concentration ($[Food]_{External}$, units defined in Table 3.1) multiplied by water inflow (V_{in}/t, in $m^3.d^{-1}$):

$$MF_{Food\_in} = [Food]_{External} \; . \; V_{in}/t \; . \; M3toL \qquad \text{(Eq. 3.2)}$$

MF_{Phyto_Growth} (Eq. 3.3) stands for the primary production in the nursery system (if applicable), which is given by the phytoplankton specific growth rate ($Growth_{phyto}$, d^{-1}) multiplied by the phytoplankton mass inside the nursery:

$$MF_{Phyto\_Growth} = Growth_{phyto} \, . [Food]_{nursery} \, . V_{nursery} \, . fraction_{phyto/food} \; . \; M3toL \qquad \text{(Eq. 1.3)}$$

Whereby $[Food]_{nursery}$ (units defined in Table 3.1) is the food concentration inside the nursery, $V_{nursery}$ (m^3) is the nursery water volume and $fraction_{phyto/food}$ is the fraction of phytoplankton in

the food. For the cases where the food indicator is phytoplankton $fraction_{phyto/food}$ is one, for the cases where the food indicator is POM or POC the average fraction of phytoplankton in the food must be defined.

MF_{Food_out}, (Eq. 3.4) is given by $[Food]_{nursery}$ multiplied by the water outflow (V_{out}/t, *in* $m^3.d^{-1}$):

$$MF_{Food\_out} = [Food]_{nursery} \; . \; V_{out}/t \; . \; M3toL \qquad \text{(Eq. 3.4)}$$

$MF_{Food\_Cleared}$ (Eq. 3.5) is given by the $[Food]_{nursery}$ multiplied by the water volume cleared by the standing stock in a given period of time ($ClearanceRate_{oyster} \; . \; Stock \; . DWtoFW \; . kg\_to\_mg$); whereby $ClearanceRate_{Oyster}$ (L. mg DW^{-1} . h^{-1}) is the oyster specific clearance rate, *Stock* (in Kg) is the spat total biomass in the tanks, and *DWtoFW* (-) is the conversion ratio of dry weight:fresh weight with shell:

$$MF_{Food\_Cleared} = [Food]_{nursery} \; . \; ClearanceRate_{oyster} \; . \; Stock \; . DWtoFW \; . kg\_to\_mg \qquad \text{(Eq. 3.5)}$$

M3toL, kg_to_mg and *kg_to_g* are conversion factors for unit consistency in Eq. 3.2 to Eq. 3.6.

The generic model solution for the questions that this work aims to address is given by Eq. 3.6 and Eq. 3.7. These are obtained by considering $V_{out}/t = V_{in}/t$ and replacing Eq. 3.2 to Eq. 3.5 into Eq. 3.1 and solving the mass balance in order to the external food concentration (Eq. 3.6) and in order to stock biomass (Eq. 3.7):

$$[Food]_{External} = [Food]_{nursery}.\left(1 - Growth_{phyto} \; . \frac{V_{nursery}}{V_{in}/t} . \; fraction_{phyto/food} + \frac{ClearanceRate_{oyster}}{V_{in}/t} . Stock. DWtoFW. kg\_to\_g\right) \qquad \text{(Eq. 3.6)}$$

$$\text{Stock} = \frac{[\text{Food}]_{\text{External}}.\text{V}_{\text{in}}/\text{t}+[\text{Food}]_{\text{nursery}}.(\text{Growth}_{\text{phyto}}.\text{V}_{\text{nursery}}.\text{fraction}_{\text{phyto/food}}-\text{V}_{\text{in}}/\text{t})}{[\text{Food}]_{\text{nursery}} \; .\text{ClearanceRate}_{\text{oyster}} \; .\text{DWtoFW} \; .\text{kg\_to\_g}} \qquad \text{(Eq. 3.7)}$$

Because of the steady-state assumption, the $[Food]_{nursery}$ is a constant; whereby the sinks and sources of the mass balance are solved to ensure that concentration in the nursery system. That parameter ($[Food]_{nursery}$) is used in the model as the optimum concentration to maintain in the production unit. Depending on the available data it can be parameterized as the minimum food concentration that maximizes ingestion or as the optimum concentration for growth. Winter (1978) argues that bivalve's filtration efficiency depends on food concentration, whereby *"From a low threshold concentration (A) onwards, filtration rate increases rapidly and is then kept constant up to a food concentration (B) at which a maximum amount of food is ingested. As soon as this maximum ingestion rate is reached, the filtration rate decreases continuously in such a way that the amount of food ingested is kept constant …. This pattern remains unchanged until*

the food concentration (C) is reached at which the production of pseudofaeces begins. At still higher food concentrations (higher than C) however, filtration and ingestion rate are drastically reduced". Thus, this is a key model parameter which allows to impose a minimum concentration that optimizes growth. All the model parameters are systematized in Table 3.2. Other key aspect for model generalization in a simple mass balance while ensuring relevant outputs is the definition of the $ClearanceRate_{Oyster}$ as a function of seed weight and water temperature (Eq. 3.8) which must be parameterized per species (or if data is available for a strain within a line):

$$\mathrm{ClearanceRate_{oyster}} = \mathrm{f(WaterTemperature, SeedWeight)} \quad \text{(Eq. 3.8)}$$

Table 3.2 - List of model parameters.

Parameter type		Parameter (Unit)	Description
Farm parameters	General settings	$V_{nursery}$ (m^3)	Water volume of the nursery. The boundaries of the system can be the volume encompassed by e.g. the flupsy area or can further include adjacent ponds for naturally grown phytoplankton communities.
		TurnoverRate (day^{-1})	Number of volume renewals per day. Should be consistent with the system boundary.
		WaterTemperature (°C)	An average value should be provided. Temperature inputs are limited to the range between 4°C and 30°C.
		$SeedWeight_{PerGrade}$ (g)	
		Food indicator	To choose from Table 3.1.
	Model solved for $[Food]_{External}$	$Stock_{PerGrade}$ (kg)	Stock biomass per grade.
	Model solved for *TotalStock*	$Stock\%_{PerGrade}$ (-)	Fraction of the stock for a given grade relative to the total biomass.
		$[Food]_{External}$	Typical external food concentration or feed supplementation. The model implementation allows testing of two values. Units depend on the food indicator chosen (Table 3.1).
Biological param. (advanced)	Species-specific	$[Food]_{nursery}$	Optimum food concentration for oyster filtration. Units depend on the food indicator chosen (Table 3.1).
		DWtoFW (-)	Conversion ratio of dry weight:fresh weight with shell.
		$ClearanceRate_{Oyster}$ (L. mg DW^{-1} . h^{-1})	The clearance rate is a model parameter that in fact is a function of seed weight and water temperature and is species-specific.
	Site specific	$Growth_{phyto}$ (day^{-1})	Specific local phytoplankton community growth rate. If values are not known a range within two values can be tested.
		$fraction_{phyto/food}$ (-)	Average typical values of the fraction of phyto in the food applicable for the cases where food indicator is POM or POC. When food indicator is algae this parameter is one.

For a practical application of this model the user can define V_{in}/t as flow rate or by the operational turnover rate (*TurnoverRate* , d^{-1}) multiplied by the nursery volume (Eq. 3.9):

$$\mathrm{V_{in}/t} = \mathrm{TurnoverRate} \,.\, \mathrm{V_{nursery}} \quad \text{(Eq. 3.9)}$$

To be useful for real farms the model was extended to consider the simultaneous cultivation of several spat grades:

i) Eq. 3.10 to estimate required external food concentration considering the summation of the volume cleared per grade ($\sum ClearanceRate_{Oyster\_PerGrade} . Stock_{PerGrade}$):

$$[Food]_{External} = [Food]_{nursery}.(1 - Growth_{phyto} . \frac{V_{nursery}}{V_{in/t}} . fraction_{phyto/food} + \frac{\sum ClearanceRate_{Oyster\_PerGrade}.Stock_{PerGrade}}{V_{in/t}} . DWtoFW . kg\_to\_g) \quad \text{(Eq. 3.10)}$$

ii) Eq. 3.11 to estimate the total maximum stock (*TotalStock*, in kg) considering a weighted clearance rate ($\sum ClearanceRate_{Oyster\_PerGrade} . Stock_{\%PerGrade}$):

$$TotalStock = \frac{[Food]_{External}.V_{in/t} + [Food]_{nursery}.(Growth_{phyto}.V_{nursery}.fraction_{phyto/food} - V_{in/t})}{[Food]_{nursery} . \sum ClearanceRate_{Oyster\_PerGrade}.Stock_{\%PerGrade} . DWtoFW . kg\_to\_g} \quad \text{(Eq. 3.11)}$$

Also for usability issues and to provide outputs of interest to farmers the final model equations (Eq. 3.10 and Eq. 3.11) are solved for two values of phytoplankton growth ($Growth_{phyto}$) and two values of external food concentration ($[Food]_{External}$). With this approach, the outputs encompass the range of scenarios within which a nursery operates, given that these two parameters are highly variable within a day.

As a case study, this model is herein applied to the Pacific oyster. Parameterization for this species is presented in Table 3.3.

Model parameterization and evaluation for the Pacific oyster

$[Food]_{nursery}$, *DWtoFW* (-), $ClearanceRate_{Oyster,}$ are species-specific and were parameterized (Table 3.3) for the Pacific oyster based on published data of spat growth experiments.

$[Food]_{nursery}$ was parameterized for the Pacific oyster spat based on Tamayo et al. (2014) which tested three feed concentrations (0.5, 3, and 6 $mm^3.L^{-1}$); the medium level was chosen given it corresponded to the highest clearance rate (for the biological meaning of $[Food]_{nursery}$ see the *Conceptual model description* section). That concentration level (which converts to 44 algal cells.μL^{-1} as per rationale explained herein) is comparable with the range indicated by Walne (1972) as the optimum for growth, around 30 to 40 algal cells.μL^{-1}. Tamayo et al. (2014) provides the conversion of the algal biovolume into POM (Particulate Organic Matter) and POC (Particulate Organic Carbon). Conversion into mg algal.L^{-1} considered that the algal cell has the same density of water following Suthers & Rissik (2009). For converting the biovolume ($mm^3.L^{-}$

^{1}) into algal cell count (algal cells.µL^{-1}) the average cell biovolume for the species used in the work by Tamayo et al. (2014), *Isochrysis galbana* Parke, of around 68 µm^{3}.cell^{-1} (Ishiwata et al. 2013) was considered. Finally, conversion into Chl-*a* was carried out using the general conversion ratio of C:Chl-*a* of around 50 (Reynolds 2006). All values are shown in Table 3.3.

Gerdes (1983a) carried out a set of experiments to study clearance rates of small size oysters ranging from 0.005 to 0.811 g DW and considering 3 different algal concentrations (50, 75, 100 cells. µL^{-1}). Herein the clearance rate allometric function defined by Gerdes (1983a) is used for a food concentration around 50 cells. µL^{-1} (see function in Table 3.3), given this is the concentration nearest to the assumption adopted in the model for $[Food]_{nursery}$ (around 44 cells. µL^{-1}, Table 3.3). For conversion between tissue dry weight and oyster total fresh weight it was considered i) the value from Gerdes (1983b) of shell weight of about 97.3% of total dry weight and ii) an average conversion factor of live fresh weight to total dry weight of around 0.5 based on Walne & Millican (1978). The resulting ratio of dry tissue weight: total fresh weight *(DWtoFW*) is around 0.014 (Table 3.3). The effect of temperature on clearance rate is included in this model based on a function by Bougrier et al. (1995) as in Table 3.3. Bougrier function for clearance rate (l.h^{-1}) is $[a-(b*(T-c)^2)]*DW^d$, whereby *a* and *b* are constants and *c* is the temperature that corresponds to maximum clearance rate (*a*=4.825, *b*=0.013, *c*=18.954; Bougriet et al. 1995). Bougrier allometric function with the temperature effect was converted into a dimensionless function to account only the effect of temperature, by dividing this general form by the function at optimum temperature (thus $T = c$). The resulting temperature dependence function $[1-a/b*(T-c)^2]$ is herein multiplied by the CR_W (equal to $CR_{W,T}$ in Table 3.3) and defines the following behavior: i) the temperature for maximum clearance rate is around 19°C, which is within the range from other references for Pacific Oyster e.g. literature revision by Barret (1963) indicates optimum around 20 °C; and ii) the clearance rate at 5°C is about 50% of the clearance rate at 20°C, which is supported by findings by Walne (1972). According to Barrett (1963) around 3°C the Pacific oyster ceases feeding so the lower limit for model input for temperature is set to 4°C. The higher temperature limit for model input was set to 30°C.

Table 3.3 - Model parameterization for Pacific oyster (*Crassostrea gigas* Thunberg).

Parameter		Value/function	Source
$[Food]_{nursery}$	(mm^3 algae.L^{-1})	3.0	Tamayo et al. (2014)
	(algal cells.μL^{-1})	44	Tamayo et al. (2014) and cell biovolume from Ishiwata et al. (2013)
	(mg algae.L^{-1})	3.0	Tamayo et al. (2014) and conversion factor from Suthers & Rissik (2009)
	(µg Chl-*a*.L^{-1})	12.5	Tamayo et al. (2014) and conversion factor from Reynolds (2006)
	(mg POM.L^{-1})	1.037	Tamayo et al. (2014)
	(mg POC.L^{-1})	0.63	Tamayo et al. (2014)
$ClearanceRate_{Oyster}$	(ml. mg DW^{-1} . h^{-1})	$CR_{W,T}$ / ($SeedWeight_{PerGrade}$ * DWtoFW *1000)	
Individual clearance rate as a function of:			
Seed weight - CR_W	(ml. h^{-1})	17.8*TissueDryWeight(mg)$^{0.79}$	From Gerdes (1983a) for a feed concentration of 50 cells. μL^{-1}
Seed weight and temperature (T) - $CR_{W,T}$	(ml. h^{-1})	CR_W*[1-0.002694*(T-18.954)^2]	Based on Bougrier et al. (1995)
DWtoFW	(-)	0.014	Gerdes (1983b); Walne and Millican (1978)

The model was evaluated using data presented by Langton & McKay (1976). Langton & McKay (1976) experiments include feed supply at two levels: i) daily supply of 180 algal cells. μL^{-1} x 250 L tank in Exp A, and ii) 120 algal cells. μL^{-1} x 250 L in Exp B. Each daily algal cell concentration (Exp A and B) is supplied following four feeding regimes (ranging from all feed supplied at once or distributed continuously over 1 day). The model is herein applied to simulate the feeding regime that provides the 2 feeding levels with a 6h interval. Within this regime the feed is supplied in a concentration (180/4 = 45 algal cells. μL^{-1}; 120/4 = 30 algal cells. μL^{-1}) that is most similar to the $[Food]_{nursery}$ set in the model (44 algal cells. μL^{-1}, Table 3.3). To mimic the experimental setting the model application includes only a single oyster grade whereby in each model run the seed size is set to the same size obtained by Langton & McKay (1976) weekly observations for the 6h on 6h off feeding regime (values taken from plots presented in Fig.1 and Fig.2 in Langton & McKay 1976). The stock biomass was calculated considering the density of 50 spat per liter multiplied by the tank volume (250 L) and by the seed size. An average temperature of 21°C was considered. A summary of the parameters used to drive the model that simulates Langton & McKay (1976) experiments are presented in Table 3.4. The model outputs for food requirement and maximum stock considering the settings for each of Langton & McKay (1976) experiments were compared with the feed given and stock of tanks and are presented in the Results section and in Table 3.6. The indication or not of food limitation was compared with the experimental outcomes and discussion carried out by of Langton and McKay (1976).

Table 3.4 - Model settings to simulate Langton & McKay (1976) experiments.

Model setting to simulate Langton & McKay (1976) experimental conditions at:								
	Week 0		**Week2**		**Week 3**		**Week 6**	
	Exp A	**Exp B**	**Exp A**	**Exp B**	**Exp A**	**Exp B**	**Exp A**	**Exp B**
$V_{nursery}$ (m^3)	0.25							
TurnoverRate (day^{-1})	1							
WaterTemperature (°C)	20.5							
Food indicator	algal cells.μL^{-1}							
$[Food]_{nursery}$	Pacific oyster parameterization (in Table 3.3)							
DWtoFW (-)								
$ClearanceRate_{Oyster}$								
$Growth_{phyto}$ (day^{-1})	0							
$fraction_{phyto/food}$ (-)	1							
SeedWeight (mg)*	0.75		4		6	5	19	11
Estimated stock (g) in the 250 L tanks	9.4		50		75	63	238	138
Feed given ($[Food]_{External}$) algal cells.μL^{-1}	180	120	180	120	180	120	180	120

* Wet weight taken from plots shown in Fig.1 (Exp A) and Fig.2 (Exp B) of Langton & McKay (1976) for feeding regime 6h on:6h off.

Model application and user interaction

For widespread use the model described herein for Pacific oyster nurseries is made available online: http://seaplusplus4.com/oysterspatbud.html. It simulates enclosed nursery systems, which include several typologies of nurseries such as a FLUPSY or land-based nurseries as reviewed by Helm & Bourne (2004). Nurseries that are interconnected with large natural blooming ponds (Helm & Bourne 2004) are also simulated, since the mass-balance includes, as an option, a source of food due to phytoplankton primary production. This model does not simulate field nursery systems, e.g. spat floating bags sitting in intertidal areas of coastal ecosystems.

Herein are described the model user interface (Figure 3.2), including the menus for nursery setup (Figure 3.3), output for food requirements (Figure 3.4), output for optimum stock (Figure 3.5), advanced settings (Figure 3.6). Examples on how to use the model for different case studies are also provided.

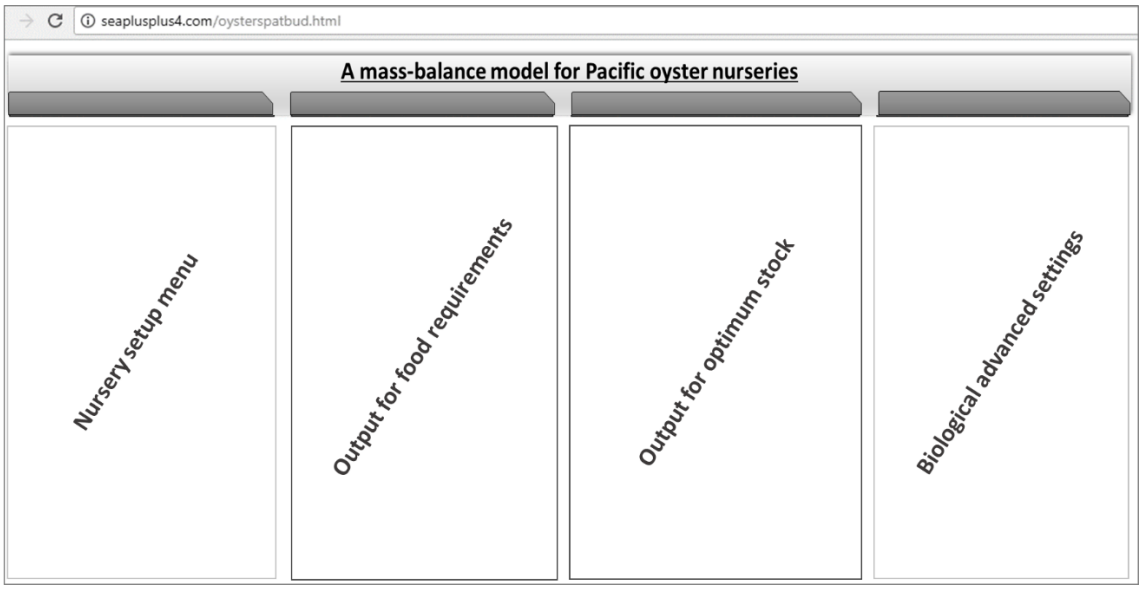

Figure 3.2 - Overall organization of model interface. Four menus: Nursery parameters, Output for food requirements, Output for optimum stock, Biological advanced settings. Full online interface available at http://seaplusplus4.com/oysterspatbud.html.

i) The nursery setup menu (Figure 3.3), is where the users enter their farm inputs such as flow rate (or turnover rate), water volume, water temperature and if the nursery includes blooming tanks. This model simulates the nursery system as a one compartment, which means for instance, if the nursery has blooming tanks the user should insert a) in the 'System volume' the sum of the volume of the oyster holding unit and of the blooming tanks, b) in the 'Flow rate' or 'Turnover rate' the water exchange with the surrounding waterbody, and c) choose 'Yes' in "With phytoplankton blooming tanks' box. Alternatively, that user can simulate only the oyster stock pond by inserting: a) in the 'System volume' the volume of that pond, b) in the 'Flow rate' or 'Turnover rate' the water exchange with the blooming tanks, and c) choose 'No' in "With phytoplankton blooming tanks' box. If the model is used to simulate a FLUPSY in an estuary the user should insert: a) in the 'System volume' the volume of the FLUPSY, b) in the 'Flow rate' or 'Turnover rate' the water flow rate forced by the paddlewheel into the entire FLUPSY, not of the individual silos, and c) choose 'No' in "With phytoplankton blooming tanks' box. Alternatively, the user can simulate the individual silo inserting in the model its water volume and individual flow rate. Examples about system definition are provided in Table 3.5.

Table 3.5 - Examples of nursery system definition for different types of nurseries (FLUPSY, Land-based with blooming tanks and closed systems).

Type of nurseries	**FLUPSY in an estuary**		**Land-based with blooming tanks** (10% renovation with external waterbody)		**Closed system** (Renovates the water every-one day)
Simulation options:	**All system**	**Only one of the silos**	**All system**	**Only the seed holding pond**	
'System volume'	Oyster holding units	1 of the silos	Oyster holding unit + blooming tanks	Oyster holding unit	Oyster holding unit
'Flow rate' / 'Turnover rate'	'Flow rate' = flow rate forced by paddlewheel	'Flow rate' = Water flow rate into one silo	'Turnover rate' = 0.1 d^{-1}	'Flow rate' = Water flow rate from the blooming tanks	'Turnover rate' = 1 d^{-1}
'With phytoplankton blooming tanks'	No	No	Yes	No	No

Besides system definition, the nursery setup menu (Figure 3.3), is where the user inserts the average seed weight per grade. Default seed grades and average weights are provided but the user can customize any of these by changing any of the boxes under 'Oyster grades' and 'Seed weight'. 'Choose food indicator' allows the user to select his preferred food indicator for model inputs/outputs.

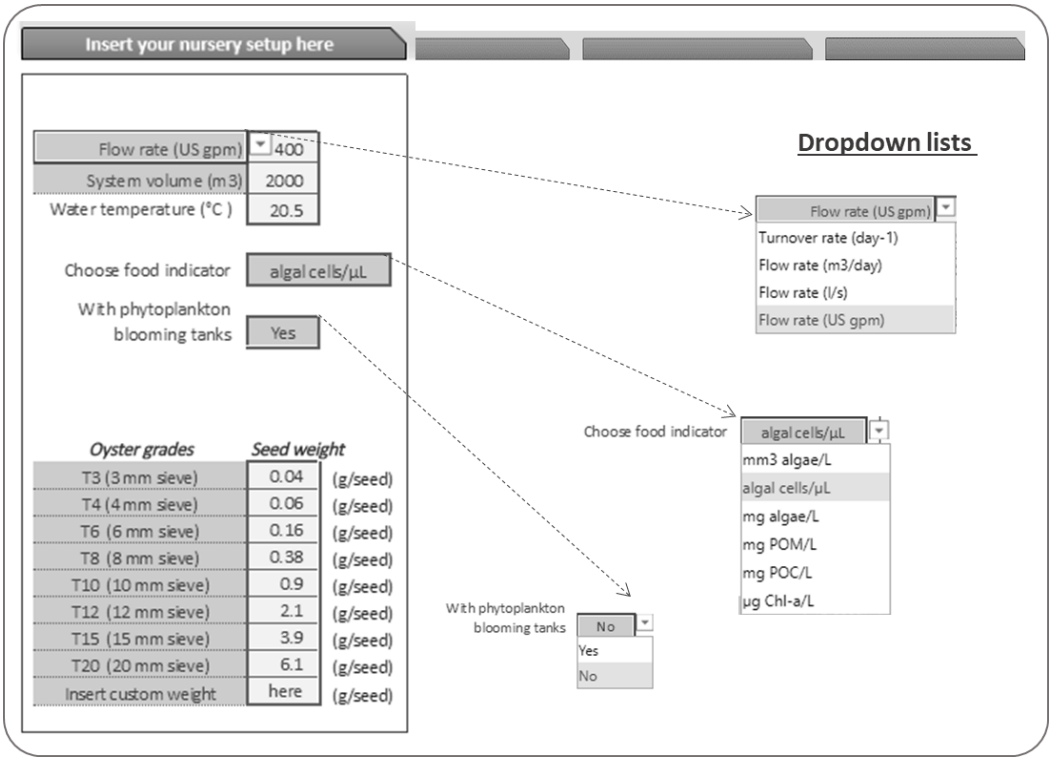

Figure 3.3 - Model interface: nursery parameters. Full online interface available at http://seaplusplus4.com/oysterspatbud.html.

ii) In the output for food requirements menu (Figure 3.4), is presented the result about the food required for a given stock, which is expressed in the units chosen by the user in the previous menu. The user should insert in this menu, below 'Stock per grade (x10^3 seeds)' the amount of seeds per grade. If the nursery includes blooming tanks then two outputs are shown that encompass a low and a high phytoplankton growth scenario (Figure 3.4).

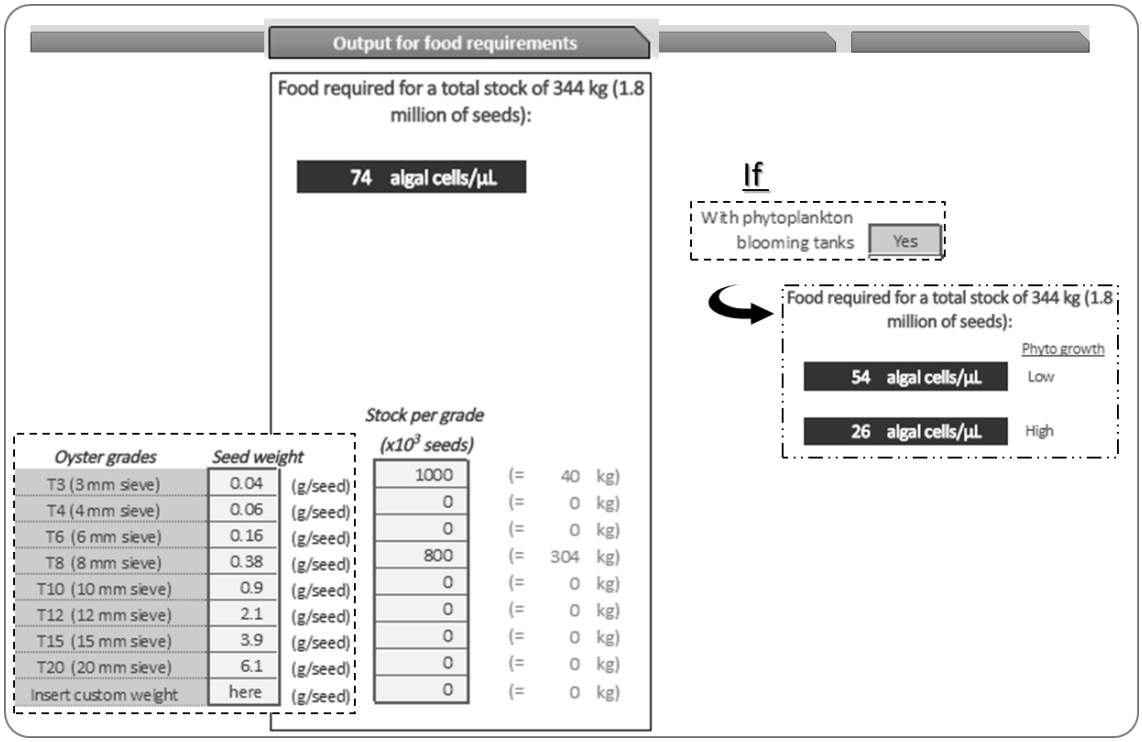

Figure 3.4 - Model interface: model outputs for minimum external food concentration for a given stock. Full online interface available at http://seaplusplus4.com/oysterspatbud.html.

iii) In the output for optimum stock menu (Figure 3.5), are presented the results about maximum stock sustained, expressed as overall biomass and as number of seeds per grade, for two scenarios of available food. The model needs to 'know' the oyster biomass distribution per grade that the farmer aims, for instance 100% of small 0.04 g spat, or 50% of the biomass stock composed of small spat and 50% composed of 0.9 spat. The user can insert that input under "Biomass % per grade" or the model calculates distribution per grade based on data about 'Stock per grade (x10^3 seeds)' inserted in the previous menu (Figure 3.4). To test the effect of different food concentration at the water intake from the surrounding ecosystem, the user must specify a lower and an upper food concentration. If the nursery includes blooming tanks then two outputs that encompass a low and a high phytoplankton growth scenario are shown for each food concentration (Figure 3.5).

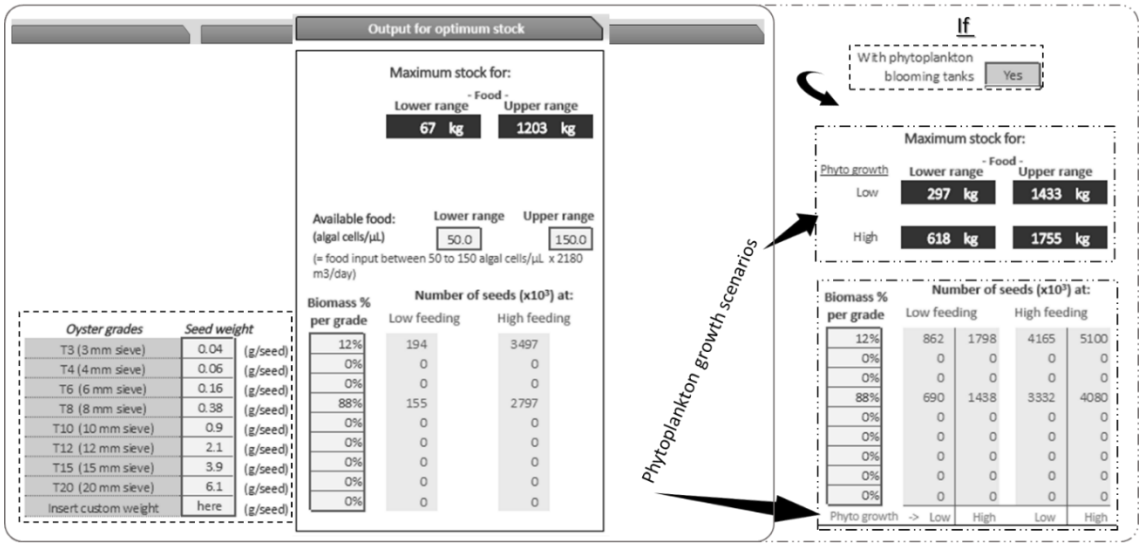

Figure 3.5 - Model interface: model outputs for maximum stock that can be sustained for a given food input and considering a given stock distribution per grades. Full online interface available at http://seaplusplus4.com/oysterspatbud.html.

iv) The advanced settings menu (Figure 3.6) allows the user to change the optimum food concentration for oyster filtration. That parameter ($[Food]_{nursery}$) is detailed in the model description and it is not foreseen that the common user will have the data required to change this value. This menu also presents the model estimates for the clearance rate based on an allometric filtration rate function (Gerdes 1983a) and the temperature dependence effect that assumes optimum filtration rate for the Pacific oyster at 19˚C (Bougrier et al. 1995). If the nursery includes blooming tanks the user can change in this menu the phytoplankton growth rate values (Figure 3.6). The model allows the user to specify a low and a high phytoplankton growth rate to test the range of community net primary production scenarios typical of the nursery's blooming tanks (Figure 3.6). Also in this menu is where the user specifies the value for the phytoplankton fraction in POM or POC, for the cases that POM or POC concentration were chosen as food indicator (Figure 3.6).

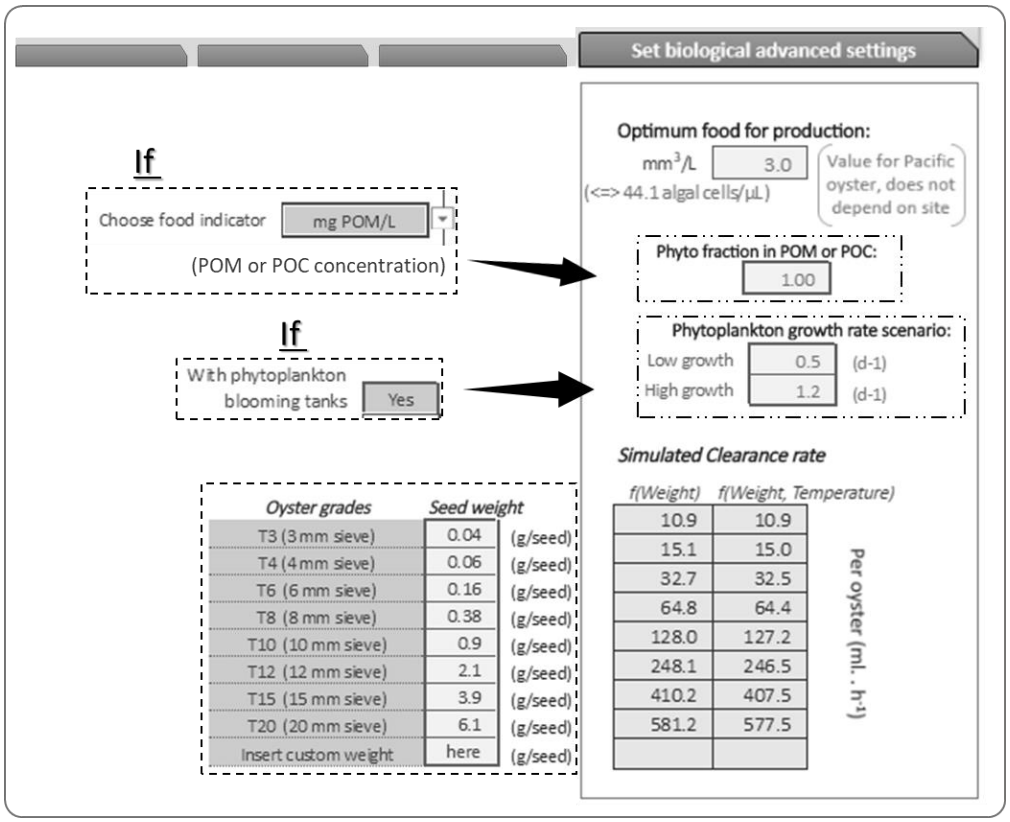

Figure 3.6 - Model interface: advanced biological parameters (user defined). Full online interface available at http://seaplusplus4.com/oysterspatbud.html.

Model limitations include:

i) Important effects that occur at a smaller scale like changes in the water flow rate due to oyster size/densities or tank shape are not simulated in the model.

ii) The option with blooming tanks assumes these are interconnected with the oyster holding tank, which together are the simulated unit. In this case the water flow is the water that enters from the outside (an adjacent ecosystem for instance) into the blooming tanks forced by tidal height or pumped.

iii) The salinity effects on filtration rate are not simulated thus it is assumed that water salinity is higher than 20.

RESULTS AND DISCUSSION

Model evaluation

The model evaluation with the Langton & McKay (1976) experiments is systematized in Table 3.4 and the results are present in Table 3.6.

For a spat of 0.75 mg and a stock of approximately 9 g in the 250 L containers, which corresponds to the conditions at the beginning (week 0) of both experiments (A - high and B - low feed level) the estimated food requirement is around 70 algal cells. μL^{-1}. For this spat weight and considering the two feed levels supplied, i.e. 180 algal cells. μL^{-1} in Exp A and 120 algal cells. μL^{-1} in Exp B, the model estimates a maximum stock of 50 g and 28 g, respectively. The outputs of this model run indicate that at week 0 the feed supplied is much higher than the stock requirements.

The model outputs for the run that simulates week 2 indicate a food requirement around 139 algal cells. μL^{-1} for the 50 g stocked in the 250 L containers (spat around 4 mg). According to this simulation outputs, the feed level supplied in Exp A is still enough, nevertheless, oysters in the containers of Exp B are fed below the optimum.

In week 3 the feed level supplied is near the threshold in Exp A and does not meet the oyster requirements in Exp B, which according to the model outputs should be 175 and 158 algal cells. μL^{-1} in Exp A and B, respectively. According to Langton & McKay (1976), the spat average weight in week 3 (6 and 5 mg in Exp A and B, respectively) already exhibit a slower growth for Exp B. In subsequent weeks the higher feed limitation experienced in Exp B (since week 2) is translated into lower weights, in week 4 spat weight is around 7.5 mg in Exp B compared with 13 mg in Exp A and by week 6 weight is around 11 mg in Exp B compared with 19 mg on Exp A (Langton & McKay 1976). These different growths measured in Exp A and B (Langton & McKay 1976) support the model predictions for food limitation. The model results also agree with the discussion of the experimental results by Langton & McKay (1976) according to which in the first 2 weeks the oyster spat are not feed limited.

Table 3.6 - Model outputs for Langton & McKay (1976) experiments.

Langton & McKay (1976) experimental conditions:		***Seed weight (mg)**	**Simulated clearance rate ($L.h^{-1}.mg\ DW^{-1}$)**	**Model outputs: Food requirements**		**Model outputs: Max stock**	
				Minimum algal cells.μL^{-1} required	*** Considering a stock (g) of:**	**Maximum stock (g)**	*** Considering a feed level (algal cells.µL-1) of:**
Week 0	**Exp A**	0.75	0.047	70	9	50	180
	Exp B					28	120
Week 2	**Exp A**	4	0.033	139	50	71	180
	Exp B					40	120
Week 3	**Exp A**	6	0.031	175	75	78	180
	Exp B	5	0.032	158	63	42	120
Week 6	**Exp A**	19	0.024	370	238	99	180
	Exp B	11	0.027	256	138	49	120

***** Settings from Langton & McKay (1976) experiments (6h on/off feeding).

Model application

The fact that the model implementation allows testing ranges of values for the external food concentration ($[Food]_{External}$) and the phytoplankton growth rate ($Growth_{phyt}$) means that model outputs provide a range of possible scenarios within which the nursery is operating. This facilitates model application into a given nursery whereby the user needs to provide the boundaries for this highly variable parameter (when dependent on food concentration in the surroundings). In extensive oyster nurseries, such seston concentration is unlikely to be monitored frequently. As such despite, the model simplification, it can still provide guidance for managing stock and food limitation in natural feeding oyster nurseries. These model functionalities contribute to support management of oyster nurseries. Namely, this model allows quantification of general rules of thumb regarding spat holding capacity for a given nursery. For instance, according with Helm & Bourne (2004) *"Determining the biomass of spat that can be held in a pond system is largely a matter of trial and error. A general rule is that 1 hectare surface area of shallow pond will support the production of between 1 and 3 tonnes biomass of seed, depending on levels of algal productivity, over the course of a growing season. This represents the maximum sustainable biomass that can be maintained with careful management"*. In order to apply the model for the described rule of thumb it is herein assumed: i) a water renovation with the external system of around 10%, ii) a system volume of about 10 000 m^3 corresponding to a surface area of 10 000 m^2 for the blooming pond + 1 000 m^2 for the stock pond and a 1 m water depth, iii) a water temperature around 19°C, iv) a phytoplankton concentration in the external waterbody within the range of about 0.5 - 2 µg Chl-*a*.L^{-1}, v) phytoplankton growth rate that ranges between 0.5 d^{-1} and 1.2 d^{-1}. The total biomass stock that can be sustained will depend on the spat grades. According with the model outputs for this setup (Figure 3.7-a) if the farmer targets to stock spat of about 0.38 g the nursery can hold in those conditions between 1 ton and 3 ton (Figure 3.7-b) of total seed biomass (corresponding to around 3 to 8 million seeds). These estimates fit well within the rule of thumb described by Helm & Bourne (2004). However, considering the same conditions but targeting to stock smaller spat of around 0.04 g the biomass stock sustained is lower (Figure 3.7-c), between 0.7 ton and 2 ton (corresponding to around 17 to 47 million seeds). The application of the model allows to improve the rule of thumb for a given set of conditions, and thus to lower the set of trials and errors required to determine the biomass of spat to hold in a pond system.

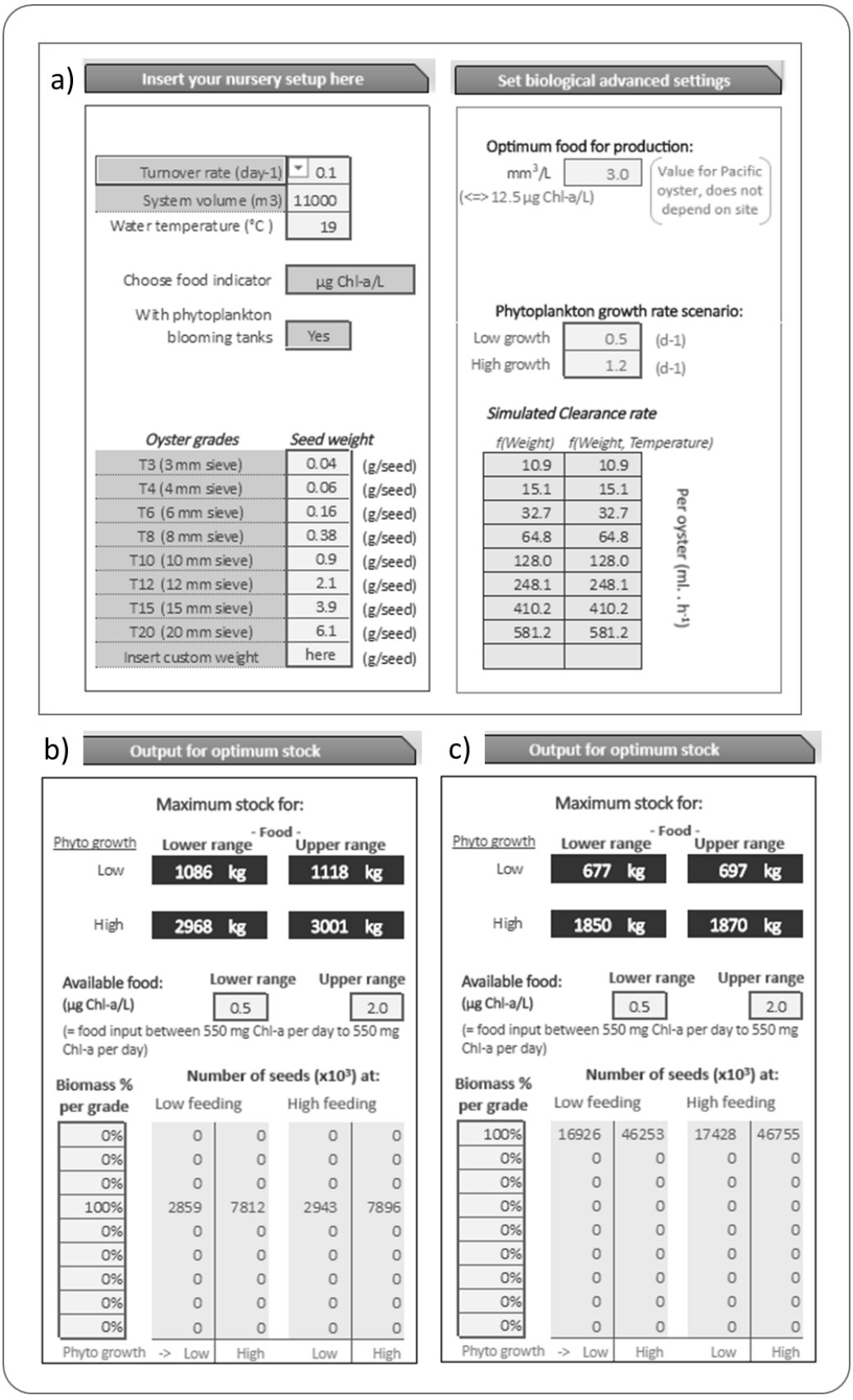

Figure 3.7 - Model application for quantification of general rules of thumb about biomass stock that can be sustained by blooming ponds: a) model setup, b) model outputs considering spat of about 0.38g, b) model outputs considering spat of about 0.04 g.

A wide range of other scenarios can be tested by any user in the online model (http://seaplusplus4.com/oysterspatbud.html) to better adjust a general rule of thumb to their own nursery conditions; for instance, and considering the abovementioned example, what are the changes regarding the stock biomass or number of seeds per grade that can be sustained due to lower or higher temperatures, typical of the local winter/summer? What if the local phytoplankton community growth rate is as low as 0.2 d^{-1}?

The inclusion in the model of a minimum concentration at the tanks that must be ensured to maximize ingestion ($[Food]_{nursery}$) is one of the key elements to solve the mass balance at the steady state. The practical implications of this assumption are that the model outputs provide i) the food requirements to ensure that minimum concentration in the nursery; considering a given water inflow, oyster filtration rate at a given stocking and seed weight, and if applicable phytoplankton natural production within the nursery; and, ii) the maximum biomass that can be stocked to ensure that minimum concentration at the nursery and thus ensure an optimized growth; considering a given food input, oyster seed weight and distribution among the oyster grades, and if applicable phytoplankton natural production within the nursery. The value adopted in the Pacific oyster model (3 $mm^3.L^{-1}$ as per rational explained in the section *Model parameterization and validation for the Pacific oyster*) was chosen from a set of 3 concentrations (0.5, 3, and 6 $mm^3.L^{-1}$) tested by Tamayo et al. (2014). It is possible that within the interval between these values other solutions maximize ingestion. Further research should be developed to more accurately estimate the $[Food]_{nursery}$. Given that other factors influence filtration efficiency dependence on food concentration, such as the algae size (Winter 1978), further research should also include different feeds. For nurseries that provide cultivated algae they can improve their own model application by changing the $[Food]_{nursery}$ parameter (in http://seaplusplus4.com/oysterspatbud.html) and inserting the value that best suits their own facility.

Nevertheless, the value adopted in the model parameterization for the Pacific oyster for the minimum food concentration that maximizes ingestion, i.e. $[Food]_{nursery}$, (44 algae cells.μL^{-1} Table 3.3) is also in agreement with experiments by Langton & McKay (1976) whereby the growth was maximized for the feed supplied (120 or 180 algae cells.μL^{-1}) with 6h interval which corresponds to 30 (=120/4) and 45 (=180/4) algae cells.μL^{-1}.

CONCLUSIONS

The mass balance model presented herein provides an assessment of the seed biomass to stock in a commercial extensive oyster nursery or for a given stock it estimates the required food. The model evaluation for the Pacific oyster using an experimental dataset (Langton & McKay 1976) indicates that it can provide valid guidance on boundaries for maximum stock at a given nursery setting or feeding requirements for a given seed stock for optimum rearing conditions. Herein it is also exemplified how to use the model to improve the application of general rules of thumb for planning oyster spat holding capacity within a nursery. The model is targeted to managers of commercial operations which are seldom the end-users of more complex approaches. Shellfish farmers are major stakeholders for the sector sustainability and thus can benefit with the application of models to manage production and understand environmental interactions, namely regarding food limitation. Further developments to the model can be made based on feedback from farmers regarding usefulness of the model, other features they find important to include, and other species.

4. A dynamic model for oyster nurseries

In this section is presented a dynamic model for oyster nurseries, developed to simulate: (i) oyster spat individual growth, (ii) food availability within the farming system, and (iii) stock biomass. This model couples an individual bioenergetic model of oyster spat, upscaled to account the population dynamics of the overall stock, with a one-compartment mass balance model.

In the first sub-sections, a description of each model component (sub-section 4.1 - 4.4) is presented, as well as the results of model validation (subsection 4.5) and sensitivity analysis (subsection 4.6). In the last, are discussed the model developments (subsection 4.7).

4.1. Oyster spat individual bioenergetic model

4.1.1. Conceptual description

The oyster spat individual bioenergetic model (Figure 4.1) was developed to simulate the growth of *Crassostrea gigas* spat. The oyster energy balance was modeled based on NEB theory, which describes the net energy balance (NEB) as the difference between energy gains and energy losses (Gosling, 2004).

$$Net\ energy\ balance\ (NEB) = energy\ gains - energy\ losses \quad \text{(Eq. 4.1)}$$

Energy gains result from food assimilation, the process that occurs after the consumption and ingestion of food. Generally, only a certain fraction of the food consumed is ingested, and the remaining fraction is rejected as pseudofaeces (Bayne, 2009). The food ingested is not all assimilated, being this process dependent, among others factors, on the quantity and quality of the food ingested (Bayne, 2017). The remaining food that is not assimilated is egested in the form of faeces. Energy losses are defined as the energy expended in metabolic activities, herein divided as standard metabolic rate and feeding catabolism. At this stage of model development excretion was not included in model formulation because it is a minor component of the oyster energy budget (Kobayashi et al., 1997; Bayne, 1999). Nevertheless, for a future use of the model, with the aim to calculate the oyster impact on the water/sediment biogeochemistry, this component must be included.

The net energy balance translates the oyster biomass variations. If the NEB is positive the energy gains are allocated to somatic growth, which will be reflected in biomass gain. If the NEB is negative the oyster will have to use energy from the reserves or the tissue, to support metabolic activities, which will be reflected in biomass loss.

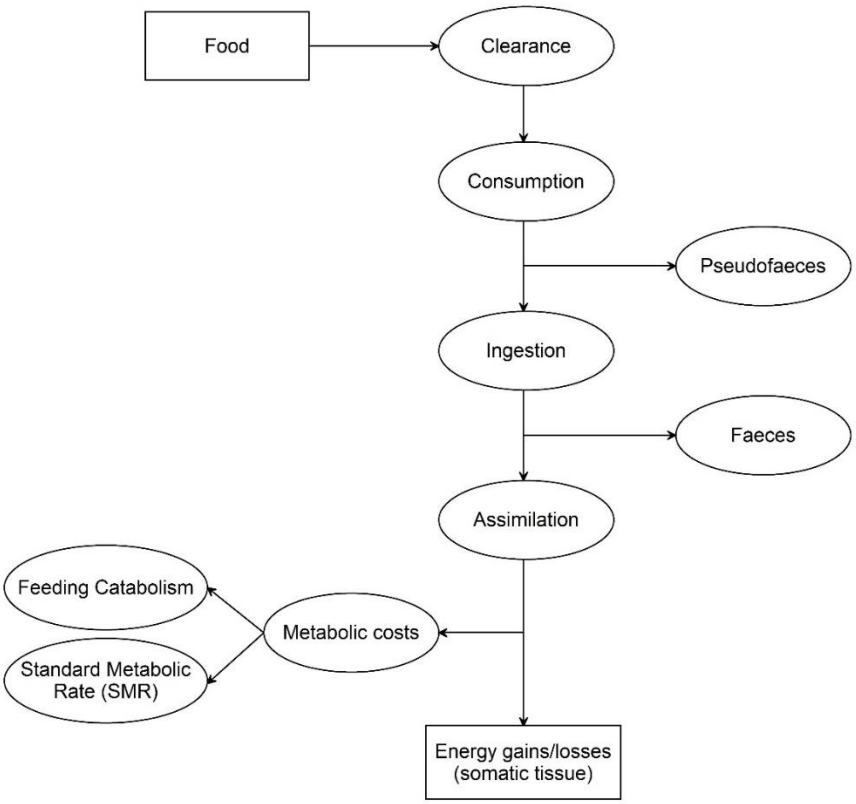

Figure 4.1 - Scheme of the oyster spat individual bioenergetic model (based on Kobayashi et al., 1997; Bayne, 1999; Gosling, 2004).

4.1.2. Model functions, parameters and conversion factors

In Table 4.1 are presented the variables, parameters, conversions factors, and functions of the model. In the next sub-sections, a description of each is made.

Table 4.1 – Variables, parameters, conversion factors and functions of the model.

Forcing Functions		
$\boldsymbol{C_{tank}}$ (cells L^{-1})		
$\boldsymbol{T}$ (˚C)		
$\boldsymbol{S}$ (psu)		
State Variables		
W_{Oyster} {g DW}		
Parameters/Conversion factors		
DWtoTFW	0.025	g DW g TFW^{-1}
CellsToChl	0.68	pg chl-*a* $cell^{-1}$
ChlToCarbon	50	g C g chl-a^{-1}
F	0.56	-

IE	0.5	-
AE	0.75	-
O2tomL	0.69978	mg O_2 ml O_2^{-1}
O2toJoule	20.08	J ml O_2^{-1}
CaloriesToJoule	4.184	J cal^{-1}
CarbonToJoule	47700	J g C^{-1}
JouleToDW	25500	J g DW^{-1}
$Costs_{feeding}$	0.55	J.J assimilated^{-1}

Functions

Food:

$$\boldsymbol{Food_{tank} = (C_{tank} \times CellsToChl \times ChlToCarbon)/10^{12}}$$

Clearance rate:

87.5 × 10^6 cells L^{-1} < $\boldsymbol{C_{tank}}$ $\quad \boldsymbol{CR_w = 14.5 \times (W_{oyster} * 1000 * f)^{0.73}/1000}$

62.5 × 10^6 cells L^{-1} < $\boldsymbol{C_{tank}}$< 87.5 × 10^6 cells L^{-1}; $\quad \boldsymbol{CR_w = 12.4 \times (W_{oyster} * 1000 * f)^{0.80}/1000}$

$\boldsymbol{C_{tank}}$< 62.5 × 10^6 cells L^{-1}; $\quad \boldsymbol{CR_w = 17.8 \times (W_{oyster} * 1000 * f)^{0.79}/1000}$

$$\boldsymbol{TF_{CR} = 1 - 0.002694 \times (T - 18.954)^2}$$

20 psu ≤ *S*; $\quad \boldsymbol{SF_{CR} = 1}$

10 psu < *S* < 20 psu; $\quad \boldsymbol{SF_{CR} = (S - 10)/10}$

S ≥ 20 psu; $\quad \boldsymbol{SF_{CR} = 0}$

$$\boldsymbol{CR_{Oyster} = CR_w \times TE_{CR} \times SE_{CR}}$$

Consumption and ingestion rates:

$$\boldsymbol{CONSUM_{Oyster} = CR_{Oyster} \times C_{tank}}$$

$$\boldsymbol{ING_{Oyster} = IE \times CONSUM_{Oyster}}$$

Assimilation rate:

$$\boldsymbol{ASSIM_{Oyster} = ING_{Oyster} \times AE \times CarbonToJoule}$$

Feeding Catabolism:

$$\boldsymbol{FEED_{Catabolism} = Costs_{feeding} \times ASSIM_{Oyster}}$$

Standard Metabolic Rate:

$$\boldsymbol{SMR_{WT} = [-0.432 + (0.613 \times 1.042^T)] \times W_{Oyster}^{0.8}}$$

20˚C ≤ *T*; $\quad \boldsymbol{TF_{SMR} = 0.0915 \times T + 1.324}$

T < 20˚C; $\quad \boldsymbol{TF_{SMR} = 0.007 \times T + 2.099}$

and

20 psu ≤ *S*; $\quad \boldsymbol{SF_{SMR} = 1}$

15 psu < *S* < 20 psu; $\quad \boldsymbol{SF_{SMR} = 1 + \{[(TF_{SMR} - 1)/5] \times (20 - S)\}}$

S ≤ 15 psu; $\quad \boldsymbol{SF_{SMR} = TF_{SMR}}$

$$\boldsymbol{SMR_{Oyster} = SMR_{WT} \times SF_{SMR} \times O2tomL \times O2toJoule}$$

Growth Rate:

$$\boldsymbol{GR_{Oyster} = (ASSIM_{Oyster} - FEED_{Metabolism} - SMR_{Oyster})/JouleToDW}$$

4.1.2.1. *Dry weight to Total Fresh Weight*

The relationship between tissue dry weight (DW) and total fresh weight (TFW) of oyster spat varies among individuals and populations (Walne & Millican, 1978; Gerdes, 1983b). Herein a constant value for conversion between DW and TFW is used. Based on Walne and Millican (1978) it was considered: (i) a mean value of shell weight of about 95%; and (ii) an average conversion factor of total fresh weight to total dry weight of around 0.5, which results in a ratio of dry tissue weight : total fresh weight (*DWtoTFW*) of around 0.025.

4.1.2.2. *Food* in the tank

The food in the tank ($Food_{tank}$, g C L^{-1}) is given by:

$$Food_{tank} = (C_{tank} \times CellsToChl \times ChlToCarbon)/10^{12} \quad \text{(Eq. 4.2)}$$

where μL_to_L and pg_to_g are conversion factors for unit consistency, and C_{tank} is the phytoplankton concentration inside the tank (expressed as cells μL^{-1}). The considered conversion factor between phytoplankton cells and ch-*a,* 0.68 ($CellsToChl$, pg chl-*a* $cell^{-1}$), was based on the median value of chl-*a* present in 8 species of phytoplankton (Table 4.2). Following Reynolds (2006), chl-*a* is multiplied by 50 ($ChlToCarbon$, g C g chl-a^{-1}) to give estimates of phytoplankton organic carbon (POC).

Table 4.2 – Chl-*a* content, by phytoplankton species, expressed as pg chl-*a* $cell^{-1}$.

Species	pg chl-*a* $cell^{-1}$	Reference
Monochrysis lutheri	0.13	Sakshaug et al. (1977)
Tetraselmis suecica	3.45	Fábregas et al. (1985)
Chlamydomonas coccoides	11.31	Montagnes et al. (1994)
Isochrysis galbana	0.17	Montagnes et al. (1994)
Pyramimonas grossi	1.05	Van Leeuwe and De Baar (2000)
Phaeodactylum tricornutum	0.09	Liu et al. (2009)
Skeletonema costatum	0.99	Hitchcock (1980)
Chaetoceros calcitrans	0.37	Phatarpekar et al. (2000)

4.1.2.3. *Clearance rate*

Clearance rate is herein defined as the volume of water filtered by the oysters. It is modeled as a function of oyster weight, water temperature, and salinity.

Gerdes (1983a) analyzed the effects of algal density on clearance rate of *Crassostrea gigas*, of the size range 0.005 - 0.811 g DW, for three concentrations of *Isochrysis galbana* (50, 75 and 100 × 10^6 cells L^{-1}) at 20˚C, and found that the amount of water filtered free of particles was in the ratio 3 : 2 : 1, respectively. Therefore, a relationship between clearance rate and tissue dry

weight were obtained for each concentration. Herein the allometric clearance rate (CR_w, L h^{-1} ind^{-1}) was modeled as:

$$\begin{aligned} &87.5 \times 10^6 \text{ cells } L^{-1} < C_{tank}; && CR_w = 14.5 \times (W_{oyster} * 1000 * f)^{0.73}/1000 \\ &62.5 \times 10^6 \text{ cells } L^{-1} < C_{tank} < 87.5 \times 10^6 \text{ cells } L^{-1}; && CR_w = 12.4 \times (W_{oyster} * 1000 * f)^{0.80}/1000 \\ &C_{tank} < 62.5 \times 10^6 \text{ cells } L^{-1}; && CR_w = 17.8 \times (W_{oyster} * 1000 * f)^{0.79}/1000 \end{aligned} \quad \text{(Eq. 4.3)}$$

where W_{oyster} is the oyster tissue dry weight (g DW). A factor *f* (Table 4.1) was included to standardize the value of tissue dry weight, in which the ratio between tissue dry weight (DW) and oyster total fresh weight (TFW) used in the model differs from Gerdes (1983a). Considering the value from Gerdes (1983b) of shell weight of about 97.3% of total dry weight and the same conversion factor of total fresh weight to total dry weight of around 0.5 (Walne & Millican, 1978), is obtained a ratio of dry tissue weight : total fresh weight ($DWtoTFW_g$) of about 0.014. Dividing this ratio, 0.014, by the dry tissue weight : total fresh weight (*DWtoTFW*) ratio used in the model, 0.025, is obtained the value 0.56, correspondent to factor *f*.

The effects of temperature on clearance rate (Eq. 4.4) were parameterized from Bougrier et al. (1995) function, obtained for oysters of the size range 0.1 - 3.0 g DW. A full explanation of this function is presented in sub-section *Model parameterization and validation for the Pacific oyster*, section 3.

$$TF_{CR} = 1 - 0.002694 \times (T - 18.954)^2 \quad \text{(Eq. 4.4)}$$

where TF_{CR} is the temperature dependent factor and *T* is the water temperature (˚C).

Studies of Quayle (1988) and Mann et al. (1994) show a decrease in relative clearance rate at salinities below 20 psu, and ceases at 10 psu. Following Kobayashi et al. (1997) the effects of salinity on clearance rate were modeled as:

$$\begin{aligned} &20 \text{ psu} \leq S; && SF_{CR} = 1 \\ &10 \text{ psu} < S < 20 \text{ psu}; && SF_{CR} = (S - 10)/10 \\ &S \geq 20 \text{ psu}; && SF_{CR} = 0 \end{aligned} \quad \text{(Eq. 4.5)}$$

where SF_{CR} is the salinity dependent factor and *S* is the water salinity (psu).

Combining Eq. 4.3, Eq. 4.4 and Eq. 4.5 is obtained the individual function of clearance rate, dependent on weight, temperature, and salinity:

$$CR_{Oyster} = CR_w \times TE_{CR} \times SE_{CR} \quad \text{(Eq. 4.6)}$$

where CR_{Oyster} is the clearance rate (L h^{-1} ind^{-1}).

A decrease of clearance rate with the increase of seston concentration was observed by several authors (e.g. Loosanoff & Tommers, 1948; Barillé et al., 1993; Ren et al., 2000; Velasco & Navarro, 2002). Although there is no specific function relying on the effects of seston concentration on clearance rate, it is assumed that the effects of phytoplankton concentration are accounted for in Eq. 4.3, defining the quantity of cells retained by the oysters. In what concerns detritus and inorganic matter the model has a limitation, due to the fact that it does not account for this fraction of seston, which may cause an overestimate on clearance rate for cases where there is a significant concentration of detritus or inorganic fractions.

4.1.2.4. Consumption and ingestion rates

Consumption rate ($CONSUM_{Oyster}$, g C h^{-1} ind^{-1}) is in here defined as the filtered food by the individual per time step:

$$CONSUM_{Oyster} = CR_{Oyster} \times Food_{tank} \quad \text{(Eq. 4.7)}$$

After consumption, and prior to ingestion, occurs a qualitative selection of the retained particles, being those with nutritive interest preferentially selected by the oyster and the non-selected particles rejected in the form of pseudofaeces (Newell & Jordan, 1983; Barillé et al., 1997; Beninger et al., 2008). As said before, the model does not enter with all the fractions of seston, so, to model the ingested fraction, it was considered that the ingestion of cells follows a constant ratio. Brown et al. (1998) analyzed ingestion rates for different microalgae species and found that for a mixed diet the oysters spat ingested 48% of the cells. Based on this value it was assumed the ratio of 0.5, correspondent to ingestion efficiency (IE), being ingestion rate (ING_{Oyster}, g C h^{-1} ind^{-1}) given by:

$$ING_{Oyster} = IE \times CONSUM_{Oyster} \quad \text{(Eq. 4.8)}$$

4.1.2.5. Assimilation rate

Gerdes (1983a) analyzed assimilation efficiencies for *Crassostrea gigas* spat and found it independent of algal concentration and body size. Average values of 72.4, 75.4 and 76.0% were obtained from those experiments. Tamayo et al. (2014) also made experiments with *Crassostrea gigas* spat and obtained assimilation efficiencies between 57.0 and 79.0%. Thus, a constant assimilation efficiency (*AE*) of 75% was used. Ingestion rate times the assimilation efficiency gives the assimilation rate ($ASSIM_{Oyster}$, J h^{-1} ind^{-1}):

$$ASSIM_{Oyster} = ING_{Oyster} \times AE \times CarbonToJoule \quad \text{(Eq. 4.9)}$$

where *CarbonToJoule* (J g C^{-1}) is the conversion factor of phytoplankton organic carbon (POC) to joule, a mean value of 47700 J g C^{-1}, obtained by converting the data present in Tab. 2 of Platt and Irwin (1973) from calories to joule using a conversion factor of 4.184 J cal^{-1}.

4.1.2.6. Metabolic costs

Oyster metabolic costs are herein divided as: Feeding catabolism, defined as the energy expended on feeding, and Standard Metabolic Rate (SMR), defined as the energy expended in the post-absorptive state (Bayne, 2017).

Physiological traits between two genetically distinct lines of *Crassostrea gigas*, slow growing and fast growing, at three level of ration were assessed by Bayne (1999). Fast growers spent less energy on feeding that slow growers. Experiments made by Tamayo et al. (2014), with oysters between the size range 0.054 - 1.955g TFW, suggests the same relationship, being these costs quantified as 0.179 and 0.592 J per joule absorbed from food, for fast and slow growers respectively. A constant value of 0.55 J.J $assimilated^{-1}$ was considered as the costs of feeding ($Costs_{feeding}$, J.J $assimilated^{-1}$), being the feeding catabolism ($FEED_{Catabolism}$, J h^{-1} ind^{-1}) modeled as:

$$FEED_{Catabolism} = Costs_{feeding} \times ASSIM_{Oyster} \quad \text{(Eq. 4.10)}$$

Assuming that the oxygen consumption of *Crassostrea gigas* spat follows the same trend of adult oysters (Gerdes, 1983b), it was used, to express the standard metabolic rate (SMR), the weight and temperature dependent function obtained by Bougrier et al. (1995):

$$SMR_{WT} = [-0.432 + (0.613 \times 1.042^{T})] \times {W_{Oyster}}^{0.8} \quad \text{(Eq. 4.11)}$$

where SMR_{WT} (mg O2 h^{-1} ind^{-1}). Despite this equation being translating herein the standard metabolic rate, in the experiments of Bougrier et al. (1995) the oxygen consumption was measured after one day of starvation, which may not be a representative period for the oysters to reach the postabsorptive state (García-Esquivel et al., 2002). Thus, it is considered that this fraction of metabolism is slightly overestimated.

To include the effects of salinity on the standard metabolic rate, the function presented by Kobayashi et al. (1997) was used:

$$\begin{aligned} &20^{\circ}C \leq T; && TF_{SMR} = 0.0915 \times T + 1.324 \\ &T < 20^{\circ}C; && TF_{SMR} = 0.007 \times T + 2.099 \end{aligned} \quad \text{(Eq. 4.12)}$$

where TF_{SMR} is the ratio of SMR at 10 psu to SMR at 20 psu: $SMR_{ST} = SMR_{10psu}/SMR_{20psu}$, and:

20 psu ≤ S;	$SF_{SMR} = 1$	
15 psu < S < 20 psu;	$SF_{SMR} = 1 + \{[(TF_{SMR} - 1)/5] \times (20 - S)\}$	(Eq. 4.13)
S ≤ 15 psu;	$SF_{SMR} = TF_{SMR}$	

Combining equation Eq. 4.11, Eq. 4.12 and Eq. 4.13 is obtained the individual standard metabolic rate (SMR_{Oyster}, J h^{-1} ind^{-1}):

$$SMR_{Oyster} = SMR_{WT} \times SF_{SMR} \times O2tomL \times O2toJoule \quad \text{(Eq. 4.14)}$$

where $O2tomL$ (0.69978 mg O_2 ml O_2^{-1}) is the conversion factor used to convert oxygen from milligrams to milliliters (Weber et al., 2008), and $O2toJoule$ (20.08 J ml O_2^{-1}) the oxycaloric coefficient to convert milliliters of oxygen into joule (Gnaiger, 1983).

4.1.2.7. Growth Rate

Growth rate (GR_{Oyster}, g DW h^{-1}) was defined as the difference between energy intake and energy expenditures:

$$GR_{Oyster} = (ASSIM_{Oyster} - FEED_{Metabolism} - SMR_{Oyster})/JouleToDW \quad \text{(Eq. 4.15)}$$

where $JouleToDW$ (= 25500 J g DW^{-1}) is a mean value of oyster energy density, obtained by converting the value 6100 cal g DW^{-1} (Cummins & Wuycheck, 1971) from calories to joule, using a conversion factor of 4.184 J cal^{-1}.

4.2. Simulation of the food concentration in the nursery

An unsteady-state one-compartment mass balance model (Figure 4.2) is herein described. The purpose of this model is to simulate the food concentration in the production tank (C_{tank}, expressed as mass per volume) as a function of the food inputs (sources) and outputs (sinks). The food sources include: (i) the food mass inflow (MF_{in}, expressed as mass per time), which can represent the food input from the sea inflow to the production tank, the food input from the water inflow of an adjacent blooming phytoplankton tank or direct feed input (*e.g.* cultured microalgae); and (ii) the phytoplankton growth in the tank (MF_{gr}, expressed as mass per time), when applicable. The food sinks include: (i) the food mass outflow (MF_{out}, expressed as mass per time), which can represent the food mass in the water discharged to the sea, to the coastal ecosystem or to an adjacent recirculation tank (*e.g.* blooming phytoplankton tank); and (ii) the food filtered by the oyster spat (MF_{cons}, expressed as mass per time).

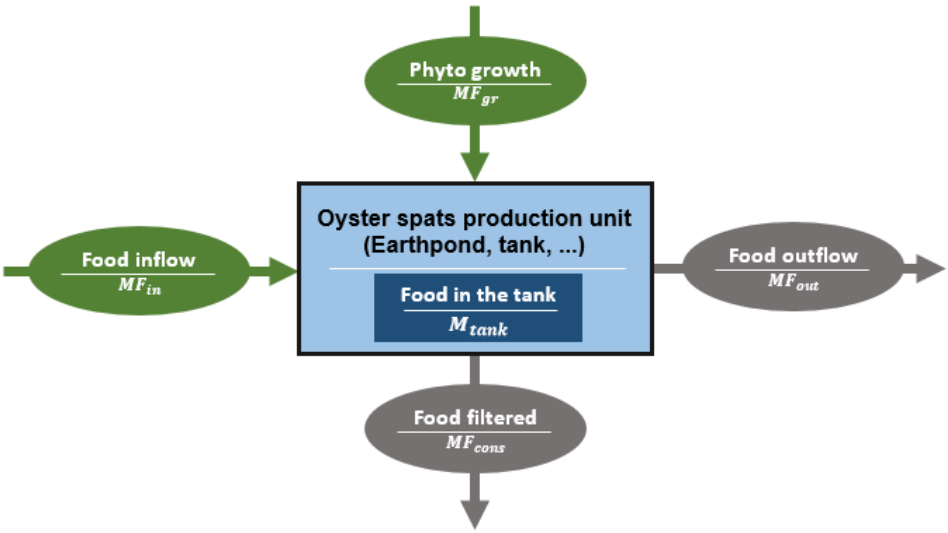

Figure 4.2 - Conceptual food mass balance model for an oyster spat production unit, where M_index represents mass and MF_{index} represents mass flows (based on Chapra, 1997).

The food concentration inside the tank is expressed here as phytoplankton cells per liter (C_{tank}, cells L^{-1}), and is obtained from:

$$C_{tank} = \frac{M_{tank}}{V_{tank} \times m3toL} \quad \text{(Eq. 4.16)}$$

where M_{tank} is the food mass in the tank (cells), V_{tank} is the tank volume (m^3) and $m3toL$ a conversion factor.

Assuming a constant tank volume, the food concentration only changes with a variation in the food mass in the tank. Following Chapra (1997), this mass variation equals the difference between the mass inputs and the mass outputs, which can be written as:

$$\frac{\mathrm{d}M_{tank}}{\mathrm{d}t} = MF_{in} + MF_{gr} - MF_{out} - MF_{cons} \quad \text{(Eq. 4.17)}$$

The food mass inflow (MF_{in}, cells h^{-1}) is given by:

$$MF_{in} = C_{in} \times \frac{V_{in}}{t} \quad \text{(Eq. 4.18)}$$

where C_{in} is the water inflow food concentration (cells L^{-1}) and V_{in} is the water inflow volume (L). As the tank volume remains constant, the water inflow rate (V_{in}/t, L h^{-1}) equals the water outflow rate (V_{out}/t, L h^{-1}), which allows to translate V_{in} as a function of the water renewal rate ($Renewal_{tank}$, day^{-1}):

$$Renewal_{tank} = \frac{V_{in}}{V_{tank} \times m3toL \times t} \times DaystoHours \quad \text{(Eq. 4.19)}$$

where $DaystoHours$ is a conversion factor for unit consistency.

Combining Eq. 4.18 and Eq. 4.19 the food mass inflow can be re-written as:

$$MF_{in} = \frac{Renewal_{tank}}{DaystoHours} \times V_{tank} \times m3toL \times C_{in} \quad \text{(Eq. 4.20)}$$

Considering a constant phytoplankton specific growth rate ($Phyto_{GrowthRate}$, day^{-1}) and a photoperiod of 12 hours ($Photoperiod_{duration}$), the food mass input due to phytoplankton growth (MF_{gr}, cells h^{-1}) was modeled as:

$$\begin{aligned} &\cos\left(2 \times \pi \times \frac{time\_step}{24}\right) \leq 0; \qquad MF_{gr} = C_{tank} \times \frac{Phyto_{GrowthRate}}{Photoperiod_{duration}} \\ &\cos\left(2 \times \pi \times \frac{time\_step}{24}\right) > 0; \qquad MF_{gr} = 0 \end{aligned} \quad \text{(Eq. 4.21)}$$

where $time\_step$ corresponds to the simulated time step, defined in hours.

The food mass output due to the water outflow (MF_{out}, cells h^{-1}) is represented by:

$$MF_{out} = \frac{Renewal_{tank}}{DaystoHours} \times V_{tank} \times m3toL \times C_{tank} \quad \text{(Eq. 4.22)}$$

The outputs related to food consumption are function of the number of individuals of each size class ($Stock_{individuals_i}$) and of the food consumption rate of those individuals ($CONS_{Oyster_i}$):

$$MF_{cons} = \left(\sum_{i=1}^{i=m} Stock_{individuals_i} \times CONS_{Oyster_i}\right) \quad \text{(Eq. 4.23)}$$

where *m* is the number of size classes. The evolution of the number of individuals over time is described in the following sub-section.

4.3. Model upscaling

The oyster spat individual bioenergetic model was upscaled to simulate the growth of all oyster population. First, it was assumed that all the individuals of each size class grows according with the individual model, where the initial weight is defined as the mean individual weight of the respective size class. In second, it was consider that the individuals within each size class die at a constant rate, being the variation in its number modeled as:

$$\frac{\mathrm{d}Stock_{individuals_i}}{\mathrm{d}t} = -Stock_{individuals_i} \times \frac{MortalityRate_i \times percent\_to\_ratio}{YearstoDays \times DaystoHours} \quad \text{(Eq. 4.24)}$$

where $Stock_{individuals_i}$ is the number of individuals of a size class, $MortalityRate_i$ is the mortality rate of each size class (expressed as % year^{-1}), and $percent\_to\_ratio$ and $YearstoDays$ are conversion factors for unit consistency.

Transfers between size classes occur when an individual reaches the mean individual weight of the next size class or the mean individual weight of the previous size class, for gains and losses of weight respectively. The number of individuals times the mean individual weight gives the stock weight of a size class ($Stock_{weight_i}$, kg), being the sum of all size classes weight defined as the total stock ($TotalStock_{weight}$, kg).

4.4. Model implementation

The dynamic model for oyster nurseries was implemented in Insight Maker (Fortmann-Roe, 2014), a web-based simulation and modelling tool, and presents a user-friendly interface (Figure 4.3). The model solutions are calculated by the Euler method, for a time step of 1 hour.

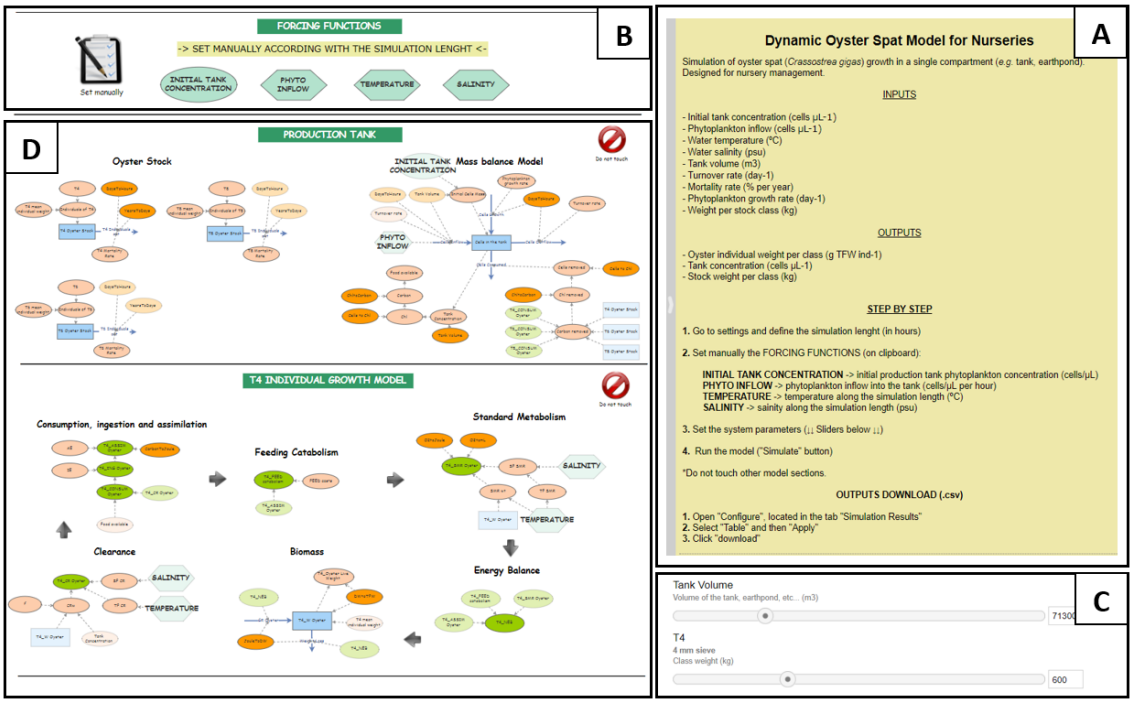

Figure 4.3 - Dynamic model for oyster nurseries, implementation snapshot: A) Comments on model application; B) Forcing functions settings (user defined); C) System parameters settings (user defined); D) Model implementation on clipboard.

4.5. Validation of the dynamic model for oyster nurseries

4.5.1. Description of the available data sets

In order to validate the dynamic model for oyster nurseries, this was run to simulate a set of experiments carried out by Langton and Mckay (1976) and by Claus et al. (1983).

Langton and Mckay (1976) tested experimentally the effects of four different feeding regimes (*i.e.* fed once a day; fed continuously; fed discontinuously with 6 h on : 6 off regime; and fed discontinuously with 3 h on : 3 h off regime) on *Crassostrea gigas* spat growth (with initial weight of about 0.25 mg DW). This experiments were run under two feeding levels of a microalgae mixture (daily supply of 180 cells μL^{-1} x 250 L per tank in Exp A and 120 cells μL^{-1} x 250 L per tank in Exp B), and carried out at ambient room temperature (19 - 22˚C), in 250 L tanks, at a density of 50 spat per liter. Filtered seawater was continuously recirculated through the individual tanks and changed every second day. The oyster spat biomass was recorded weekly along all experimental period (7 weeks for Exp A and 6 weeks for Exp B). For purposes of model application, as water temperature and salinity were not measured, a constant water temperature of 20.5˚C was assumed, corresponding to the average ambient room temperature, and a constant water salinity of 33 psu, equal to the mean Menai Strait's seawater salinity (Buchan et al., 1967).

Claus et al. (1983) recorded the growth of *Crassostrea gigas* spat, in a land-based nursery, as a function of: (i) water temperature, heated seawater at 15˚C or unheated sea water (following the aimbient temperature of Sluice Dock); and (ii) feeding level, with supply of microalgae (in the range 10 – 50 cells μL^{-1}) or without supply of microalgae. Concerning this experimental settings, four experiments were carried out by Claus et al. (1983):

- One favorable experiment (heated sea water + supply of microalgae);
- Three unfavorable experiments (heated sea water + no supply of microalgae; unheated seawater + supply of microalgae; unheated seawater + no supply of microalgae).

During the experimental period, water salinity remained at 25 psu, with minor fluctuations to 24 psu and 26 psu. The oyster spat were stocked in upflow cylinders, placed inside rearing tanks, at a density of 30 000 individuals per cylinder, each one with an approximately flow rate of 10 L min^{-1}. For purposes of model application a tank volume of 600 L was assumed, calculated as the volume that flows through the cylinder per hour. As the feeding level was expressed as a range, without a description of its variation among the experimental period, it was used a constant value during all the simulation period (Table 4.3).

4.5.2. Validation data sets

From the previously described experiments were chosen to validate the model: (i) the Exp A and Exp B for the feeding regime in continuously, from Langton and McKay (1976); and (ii) the favorable experiment of Claus et al. (1983), assuming a constant food level of 25 cells μL^{-1}, within the given feeding range (10 – 50 cells μL^{-1}). In Table 4.3 are shown the model settings for the three experimental conditions as well as the reported biomass over time, expressed as total fresh weight (TFW).

Table 4.3 – Settings of the dynamic model for oyster nurseries to simulate Langton and McKay (1976) and Claus et al. (1983) experimental conditions.

Model settings to simulate Langton and McKay (1976), and Claus et al. (1983) experimental conditions:			
	Langton & McKay (1976)		**Claus et al. (1983)**
	Exp A	**Exp B**	**Exp Favorable**
V_{tank} (m^3)	0.25		0.6
$Renewal_{tank}$ (day^{-1})*	0.5		24
$Phyto_{GrowthRate}$ (day^{-1})	0		0
$Stock_{individuals}$ (n° of individuals)	12 500		30 000
MortalityRate (% yr^{-1})	0		0
T (°C)	20.5		15
S (psu)	33		25
$C_{tank\_initial}$ (cells μL^{-1})	0		0
C_{in} (cells μL^{-1})	180	120	25
Simulation period (h)	1176	1008	2352
Timestamp:	*Oyster Biomass (g TFW)***		
Week 0	0.001	0.001	0.038
Week 1	0.002	0.002	-
Week 2	0.004	0.003	-
Week 3	0.007	0.005	0.087
Week 4	0.009	0.006	-
Week 5	0.010	0.007	-
Week 6	0.016	0.008	0.194
Week 7	0.021	-	-
Week 8	-	-	0.171
Week 14	-	-	0.410

*Model structure was changed to simulate Langton and McKay (1976) experiments. $Renewal_{tank}$ was modeled to simulate all tank volume renewal at once, every second day.
**Total fresh weight taken from plots shown in Fig. 1 (Exp A) and Fig. 2 (Exp B) of Langton and McKay (1976) for feeding regime in continuously; and from plots shown in Fig. 2 of Claus et al., (1983).

Phytoplankton growth rate ($Phyto_{GrowthRate}$), mortality rate (*MortalityRate*) and initial tank concentration ($C_{tank\_initial}$) were not considered in any simulation because they are not representative conditions of the experimental systems. Exp A and Exp B, from Langton and McKay (1976), were simulated for 7 weeks and 6 weeks, respectively, according to the experimental period. Claus et al., (1983) experiment was simulated for 14 weeks, corresponding only to 4 months (from December to March) of the experimental period. As the reported growth

was different among individuals it was chosen to simulate the individuals with an intermediate growth (see Fig. 2 of Claus et al., 1983).

The Pearson's correlation coefficient (r) and index of agreement (d_2, Willmott et al., 1985), were calculated for all datasets to evaluate model accuracy.

4.5.3. Validation outputs

A comparison between observed and simulated oyster biomass is presented in Figure 4.4, Figure 4.5 and Figure 4.6, and the statistical tests are presented in Table 4.4, for each considered dataset (see Table 4.3).

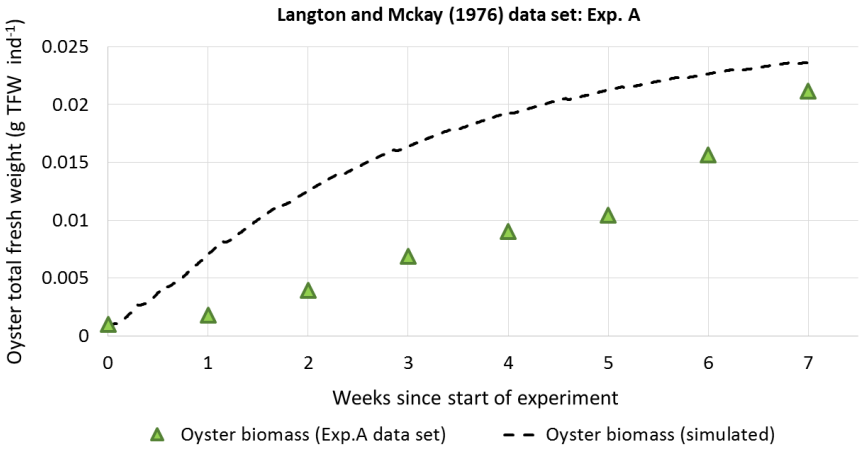

Figure 4.3 - Simulated and observed growth of *Crassostrea gigas* spat, for Exp A from Langton and McKay (1976) dataset (Table 4.3).

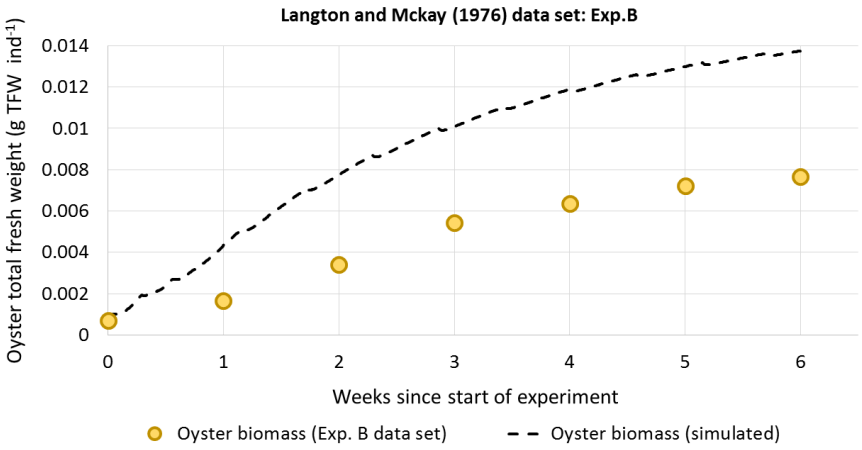

Figure 4.4 - Simulated and observed growth of *Crassostrea gigas* spat, for Exp B from Langton and McKay (1976) dataset (Table 4.3).

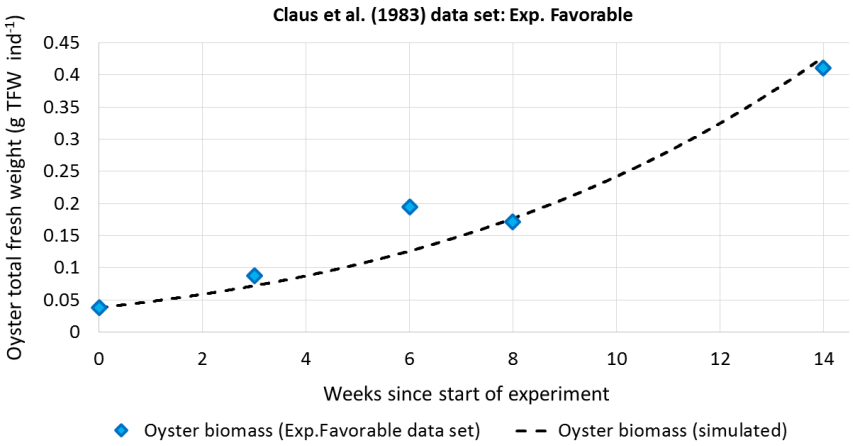

Figure 4.5 - Simulated and observed growth of *Crassostrea gigas* spat, for Exp Favorable from Claus et al., (1983) dataset (Table 4.3).

Model application, for Exp A and Exp B from Langton and McKay (1976) datasets (Figure 4.4 and Figure 4.5, respectively), shows a significant agreement (r = 0.895, n = 7. $p < 0.05$; r = 0.997, n = 6, $p < 0.05$, respectively) between the observed and simulated oyster biomass. However, both simulations overestimate the oyster biomass. For Exp A the overestimations present small differences at the start as well as at the end of the simulation, and big differences in the middle, being the final simulated oyster biomass (0.0237 g TFW) close to the observed (0.0211 g TFW). For Exp B the difference between simulated and observed values increases along the simulation period, where the final simulated biomass (0.0138 g TFW) is about 1.8 times higher than the observed (0.0077 g TFW). Despite the better model fit at the end of the simulation for Exp A, the simulated growth pattern adjusts better to Exp B.

Model application for Exp Favorable, from Claus et al. (1983), also shows a significant agreement (r = 0.976, n = 4, $p < 0.05$) between the simulated and observed oyster biomass, despite the slight underestimation at week 6 (Figure 4.6). The final simulated oyster biomass (0.4277 g TFW) is very close to the observed value (0.4102 g TFW).

Index of agreement (d_2) shows high values either for Exp A as for Exp Favorable (0.839 and 0.980, respectively, Table 4.4), which reinforce the good model fit for these data sets. The lower value of the index of agreement for Exp B (0.689, Table 4.4) can be explained by bigger differences between the simulated and observed oyster biomass in comparison with the other simulations. Nevertheless, as all the values are larger than 0.5, it can be said that the model simulations present good representations of the oyster spat growth.

Table 4.4 – Statistical tests, Pearson's correlation coefficient (r) and index of agreement (d_2).

Simulated data set*	Reference	Pearson's correlation coefficient (r)	Index of agreement (d_2)
Exp A	Langton & McKay (1976)	0.895 ($p < 0.05$)	0.839
Exp B	Langton & McKay (1976)	0.997 ($p < 0.05$)	0.689
Exp Favorable	Claus et al. (1983)	0.976 ($p < 0.05$)	0.980

*Datasets described in Table 4.3.

4.6. Sensitivity analysis of the oyster spat individual bioenergetic model

4.6.1. Overall description

A sensitivity analysis was carried out for the individual dynamic oyster model based on Majkowski (1982). In order to identify the relationship between model parameters and model outputs, each parameter was changed by minus or plus 10%. The analysis was carried out with the model settings used to simulate the Claus et al. (1983) dataset (Table 4.3, sub-section 4.5.2).

4.6.2. Sensitivity analysis results

Table 4.5 features the average changes in oyster total fresh weight derived from adjustments of plus and minus 10% for each model parameter. Average changes up to 51% (Table 4.5) indicate that the model is sensitive to the tested parameters.

Table 4.5 – Sensitivity analysis of the dynamic oyster model, for changes in plus and minus 10% on model parameters, applied for Exp Favorable from Claus et al., (1983) dataset.

Model parameter	**Value**	**Unit**	**Percentage changed in oyster total fresh weight**		
			Parameter plus 10%	Parameter minus 10%	Average of each 10% adjustment
DWtoTFW	0.025	g DW g TFW^{-1}	4%	5%	4%
CellsToChl	0.68	pg chl-*a* $cell^{-1}$	48%	35%	41%
ChlToCarbon	50	g C g chl-a^{-1}	48%	35%	41%
IE	0.5	-	48%	35%	41%
AE	0.75	-	48%	35%	41%
O2toJoule	20.08	J ml O_2^{-1}	20%	24%	22%
CarbonToJoule	47700	J g C^{-1}	48%	35%	41%
JouleToDW	25500	J g DW^{-1}	16%	23%	19%
$Costs_{feeding}$	0.55	J J $assimilated^{-1}$	41%	61%	51%

Those parameters, excluding *DWtoTFW*, are directly related with energy conversions (*CellsToChl, ChlToCarbon, O2toJoule, CarbonToJoule, JouleToDW*) and with processes that define energy inputs or intake (*IE, AE, $Costs_{feeding}$*). It is worth to note that the last were assumed in the model as constant values despite those fractions are known to be variable.

4.7. Discussion of the dynamic oyster model for nurseries

The dynamic model for oyster nurseries successfully simulated the oyster spat biomass for three data sets, despite presenting slight overestimations for two of them (sub-section 4.5). Due to the lack of datasets to validate the simulations of food in the nursery and stock biomass this assessments were not performed.

Overestimations in oyster biomass may be associated with the model sensitivity to the defined parameters. As previously highlighted, almost all those parameters translate or energy conversions or processes that define the input/intake of energy as constant ratios, which may not truly represent the reality. One important point in the model formulation is how to define both food availability and quality since these have implications in the definition of the processes related to feeding behavior and energy intake. In this model, the food is defined only as phytoplankton, which may not allow a good representation of most of the feeding related processes in systems with abundant non-phytoplankton particles.

Several authors observed a decrease in clearance rates with an increase in seston concentration (e.g. Loosanoff & Tommers, 1948; Barillé et al., 1993; Ren et al., 2000; Velasco & Navarro, 2002), and others successfully modeled those effects on *Crassostrea gigas* clearance rate (e.g. Barillé et al., 1997; Kobayashi et al., 1997). Herein, these effects are not being completely represented, being only accounted the effects of the phytoplankton concentration, which may cause an overestimation in clearance rate for the cases where there are significant concentrations of other fractions of seston (i.e. detritus and inorganic particles). There is also enough evidence that the quality of the ingested food depends on a pre-ingestive selection (Newell & Jordan, 1983; Barillé et al., 1997; Beninger et al., 2008) and that assimilation efficiencies vary with the quality of the ingested food (Gerdes, 1983a; Bayne, 2009; Tamayo et al., 2014). In the model, ingestion and assimilation efficiencies are constant ratios, what suits if food is defined only as phytoplankton. However, a great part of oyster nurseries are placed in turbid environments, including in abundance other non-phytoplankton particles. Regarding this, further developments must be done aiming the inclusion of non-phytoplankton particles in model formulation. Following this approach, faeces and pseudofaeces can also be better defined,

which together with the inclusion of excretion, will allow the calculation of oyster impact on the water/sediment biogeochemistry.

In what concerns the energy expended on feeding, it is known that is variable between slow and fast growers (Bayne, 1999; Tamayo et al., 2014). To simplify model formulation it was herein modeled as a constant fraction of the assimilated energy. In the scientific papers where the datasets were withdrawn (i.e. Langton & McKay 1976; Claus et al., 1983), the oyster weights are presented as the weight of a group of individuals or as the average individual weight of a given size class. Thus, by validating the model for these data sets, it is also considered that the individual growth model simulates the average individual. This model was upscaled to simulate the growth of the overall nursery stock, where an individual moves to an adjacent size class by reaching the mean weight of the individual of that size class. In this way, all the individuals of a certain size class move to other at the same time, thus not representing: (i) differences between fast and slow growers; and (ii) different individual weights within a size class. To account for these differences, future developments must be done aiming the inclusion of individual growth variance in the modelling of population dynamics (e.g. Gangnery et al. 2004).

Although the model is formulated with the aforementioned simplifications, necessary due to the available datasets for model validation/calibration, the model can be calibrated and parameterized for the specific system where it will be applied. For instance, the conversion factors between algal cells, chlorophyll-*a*, particulate inorganic carbon (POC), and energy (expressed in joules) can be changed to better represent a given system, e.g. for the cases where the microalgae mixture constitution is well known.

5. Model application in a commercial nursery

5.1. Application of the static mass balance model for oyster nurseries

5.1.1. Overall description

The static mass balance model for oyster nurseries was applied for four scenarios, concerning different environmental and system conditions, and four stock distributions (Table 5.1 and Table 5.2), to assess maximum stock that ensures optimum growth conditions. The stock distributions, which include four oyster size classes (T3, T4, T6 and T8, described in Table 2.1) follow the normal evolution of the stock (expressed as number of individuals per oyster size class) in Bivalvia's nursery (Table 5.1). Scenario 1 and 2 stands for the south system (SS) operation at two different renewal rates, while scenario 3 and 4 stands for the north system (NS) operation at two different temperatures, representing winter and summer conditions. These are defined as:

Scenario 1 – represents south system (SS) operating at a minimum turnover rate (0.02 day^{-1}), at 20˚C;

Scenario 2 – represents south system (SS) operating at a maximum turnover rate (0.05 day^{-1}), at 20˚C;

Scenario 3 – represents north system (NS) operating at a minimum turnover rate (0.02 day^{-1}), at 15˚C;

Scenario 4 – represents north system (NS) operating at a minimum turnover rate (0.02 day^{-1}), at 29˚C.

Table 5.1 – Stocking scenarios and distribution per oyster size class, for the application of the static mass balance model for oyster nurseries.

Stocking Distribution (SD)	***Distribution per oyster size class***			
	T3	T4	T6	T8
SD1	100%	-	-	-
SD2	75%	25%	-	-
SD3	50%	25%	25%	-
SD4	20%	25%	35%	20%

As previously described, the production tank includes phytoplankton blooming ponds. Based on experiments made by Domingues et al. (2015) a specific phytoplankton growth rate ($Growth_{phyto}$) between 0.2 and 0.9 day^{-1} was assumed for all the scenarios. External phytoplankton concentration was set to vary in the range 0.3 - 1.0 cells μL^{-1}.

Table 5.2 – Model settings for the application of the static mass balance model for oyster nurseries, for different scenarios.

Model settings for the application of the static mass balance model for oyster nurseries, for different scenarios

		Scenario 1				Scenario 2				Scenario 3				Scenario 4			
		SD1	*SD2*	*SD3*	*SD4*	*SD1*	*SD2*	*SD3*	*SD4*	*SD1*	*SD2*	*SD3*	*SD4*	*SD1*	*SD2*	*SD3*	*SD4*
$V_{nursery}$ (m^3)		55 300				55 300				71 300				71 300			
TurnoverRate (day^{-1})		0.02				0.05				0.02				0.02			
WaterTemperature (°C)		20				20				15				29			
Food indicator		cells μL^{-1}															
Phytoplankton blooming tank		yes															
$[Food]_{external}$ (cells μL^{-1})*	LR	0.3															
	UR	1															
$Growth_{phyto}$ (day^{-1})**	LG	0.2															
	HG	0.9															

*External phytoplankton concentration, expressed for a lower range (LR) and upper range (UR).

**Phytoplankton growth rate for a low growth (LG) and high growth (HG) scenario, based on Domingues et al. (2015).

5.1.2. Outputs of the static mass balance model application

Simulated maximum stocks (expressed by weight and number of individuals), for each scenario and concerning different stock distributions, are presented in Table 5.3.

According to the Table 5.3, the stock distribution 1 (SD1) only enables about half of the maximum stock weight in relation to the other stock distributions, because SD1 is totally constituted by individuals of the oyster size class T3, which: (i) have the lowest individual weight and (ii) the highest specific clearance rate. This reflects that a lower stock weight can filter about the same amount of food in comparison with a higher stock weight, distributed by higher size classes. Despite the remainder stock distributions (SD2, SD3, and SD4) presenting a variable distribution of individuals among size classes, it is interesting to see that the simulated stock weight is about the same between them, with minor variations. However, the weight does not translate the number of individuals. For all scenarios, SD2 is the stock distribution that enables rearing a higher number of individuals, and SD4 the stock distribution that enables a lower number (Table 5.3). Within each scenario, SD1 and SD3 show similar stock values (expressed as number of individuals).

Both simulations for scenario 1 and 2 present similar results. This is due to the fact that the only difference between these two scenario settings is the turnover rate value (0.02 day^{-1} for scenario 1 and 0.05 day^{-1} for scenario 2, Table 5.2). As explained before the lowest stock weights can be found for SD1, whereby for scenario 1 simulated maximum stock weights are around 1 500 and 7 500 kg, while for scenario 2 maximum stock weights are around 1 200 and 7 200 kg, for low and high feeding regimes/phytoplankton growth respectively. In what concerns highest stock weights, scenario 1 shows values near 2 500 and 13 000 kg, while scenario 2 shows values near 2 200 and 12 000 kg, for low and high feeding regimes/phytoplankton growth. For both scenario 1 and 2, the stock distribution SD2 presents the highest number of individuals (of about 270 × 10^6 individuals) and SD4 the lowest number (of about 130 × 10^6 individuals).

As would be expected, this two scenarios (scenario 1 and 2) present lower results in comparison with scenario 3 and 4, because in both simulations the water temperature was set as 20˚C, near the optimum temperature for maximum clearance rate (around 19˚C, see sub-section *Model parameterization and evaluation for the Pacific oyster*, section 3), which translates into a higher food consumption per individual.

Table 5.3 – Maximum stock, expressed by weight (kg) and number of individuals (x10^6 individuals), for each scenario concerning different stock distributions.

Maximum stock weight for each scenario by stock distribution									
Scenarios divided by feeding regime and phytoplankton growth rate*:		**Stock distribution (SD)**:**							
		SD1		*SD2*		*SD3*		*SD4*	
		kg	**x10^6 individuals**	**kg**	**x10^6 individuals**	**kg**	**x10^6 individuals**	**kg**	**x10^6 individuals**
Scenario 1	*Low*	1 522	38.1	2 632	56.9	2 507	41.8	2 618	26.5
	High	7 440	186.0	12 864	278.0	12 253	204.5	12 794	129.3
Scenario 2	*Low*	1 270	31.8	2 197	47.5	2 092	34.9	2 185	22.1
	High	7 192	179.8	12 436	268.7	11 845	197.7	12 368	125.0
Scenario 3	*Low*	2 043	51.1	3 532	76.3	3 364	56.1	3 513	35.5
	High	9 984	249.6	17 265	373.0	16 444	274.5	17 170	173.5
Scenario 4	*Low*	2 687	67.2	4 647	100.4	4 426	73.9	4 622	46.7
	High	13 136	328.4	22 714	490.8	21 634	361.1	22 589	228.3

*For all scenarios "*Low*" corresponds to a low feeding regime combined with a low phytoplankton growth rate, and "*High*" corresponds to a high feeding regime combined with a high phytoplankton growth rate;

**Stock distribution description in Table 5.1.

Looking to the food inflow as only phytoplankton, and dismissing the nutrients inflow (which have influence on phytoplankton growth rate), is possible to conclude that higher turnover rates, for the considered external concentration range (0.3 to 1 cells μL^{-1}, described in subsection 2.2.), are prejudicial for the optimization of the maximum stock. Differences between stocks of scenario 2 and scenario 1, expressed as number of individuals, suggests a decrease in the maximum stock in 4 and 20% by increasing the turnover rate (from 0.02 to 0.05 day^{-1}), for high and low feeding regimes/phytoplankton growth respectively.

Scenarios 3 and 4 were simulated considering a water temperature of 15˚C and 29˚C respectively, and different results were obtained. The lowest stock weights, correspondent to stock distribution 1 (SD1), are around 2 000 and 10 000 kg in scenario 3, and around 2 700 and 13 000 kg in scenario 4, for low and high feeding regimes/phytoplankton growth respectively. The highest stock weights, similar to SD2, SD3, and SD4, are around 3 500 and 17 000 kg for scenario 3, and around 4 500 and 22 500 kg for scenario 4, for low and high feeding regimes/phytoplankton growth. In what concerns the stock expressed as number of individuals, scenario 3 shows the highest stock for SD2 (76.3 and 373.0 × 10^6 individuals, for low and high feeding regimes/phytoplankton growth) and the lowest stock for SD4 (35.5 and 173.5 × 10^6 individuals, for low and high feeding regimes/phytoplankton growth). Also, scenario 4 presents the highest simulated stocks for SD2 (100.4 and 490.8 × 10^6 individuals, for low and high feeding regimes/phytoplankton growth) and the lowest for SD4 (46.7 and 228.3 × 10^6 individuals, for low and high feeding regimes/phytoplankton growth).

From the comparison between scenario 3 and scenario 4 seems that high water temperatures, typical of summer condition, enable the rearing of higher stocks in relation to low water temperatures, which are characteristic of the winter season. In this case, the simulated maximum stocks (expressed as number of individuals) are about 30% higher at 29˚C than at 15˚C. But this does not mean that exists a direct relationship between water temperature and the maximum stock. This relative increase, in the simulated stock, is due to clearance rate at 29˚C be about 30% lower than at 15˚C. In fact, this relation is inversely proportional to clearance rate, i.e., the lower the clearance rate the higher is the maximum stock, and vice versa. Regarding this, a relationship between the relative increase in the simulated stock and water temperature, in relation to a standard stock simulated at 19˚C (temperature for maximum clearance rate, see sub-section *Model parameterization and evaluation for the Pacific oyster*, section 3), is presented in Figure 5.1. This relationship is within the temperature limits set in the model (see section 3).

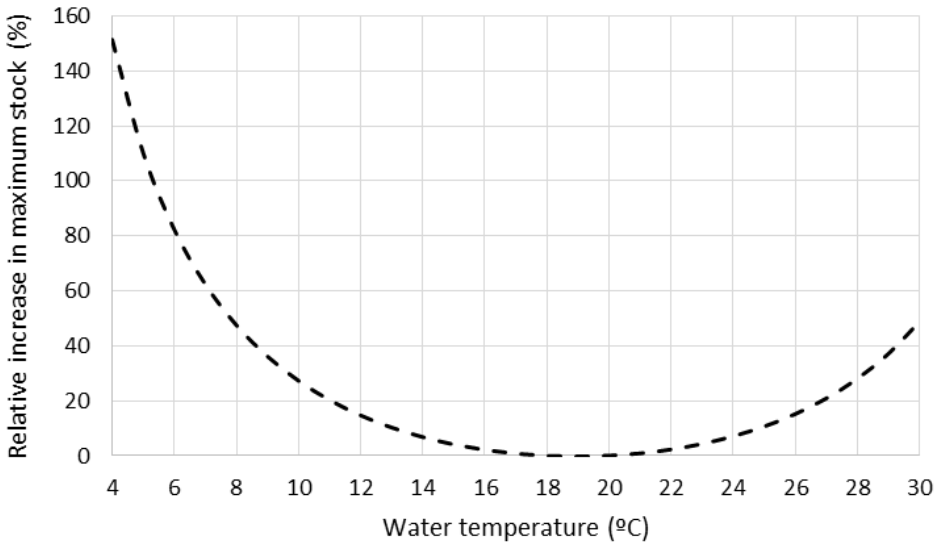

Figure 5.1 - Relative increase in maximum simulated stock due to water temperature effects, in relation to a standard stock simulated at 19˚C.

Finally, as the goal of this application is the calculation of maximum stocks for several stocks distributions, each one divided according to the normal evolution of the stock, should be considered for each scenario as the initial seeding stock (expressed as number of individuals) the correspondent to SD4. As the estimates for SD4 show the lowest stocks (expressed as number of individuals), any initial seeding stock (correspondent to SD1 in this case) above these numbers will not meet the food demands in the future, when the stock reaches the stock distribution 4 (SD4).

5.2. Application of the dynamic model for oyster nurseries

5.2.1. Overall description

The dynamic model for oyster nurseries was applied to six scenarios to compare the system behavior under different stocking, food and environmental conditions (Table 5.5). All the simulations were run for a period of 1 176 hours, correspondent to 7 weeks. Despite the commercial system operates with a large range of oyster spat size classes, it was only considered three of them (T4, T6, and T8). Scenario 1, 2, 3 and 4 represent the environmental conditions and feeding regimes of the different seasons of the year and were simulated for a total stock of 1 000 kg, while scenario 5 and 6 were simulated for a total stock of 3 000 kg, for a low and high feeding regime, with the objective to compare the system behavior under a higher stock density. These are defined as follows:

Scenario 1 – represents winter conditions, where water temperature reaches 15˚C and the initial tank concentration 150 cells μL^{-1};

Scenario 2 – represents spring conditions, where water temperature is about 25˚C and the initial tank concentration 150 cells μL^{-1};

Scenario 3 – represents summer conditions, where water temperature reaches near 30˚C and the initial tank concentration 100 cells μL^{-1};

Scenario 4 – represents autumn conditions, where water temperature is about 20˚C and the initial tank concentration 180 cells μL^{-1};

Scenario 5 – high feeding regime (initial tank concentration of 180 cells μL^{-1}) for a total stock of 3 000 kg;

Scenario 6 – low feeding regime (initial tank concentration of 100 cells μL^{-1}) for a total stock of 3 000 kg.

Initial tank concentrations ($C_{tank\_initial}$) were set based on estimates from the analyses of the system, where low phytoplankton concentrations in the summer can probably be explained by limited nutrient availability (Barbosa, 2010).

Table 5.4 – Model settings for the application of the dynamic oyster model on different scenarios.

Model settings for the application of the dynamic oyster model on different scenarios

		Scenario 1	*Scenario 2*	*Scenario 3*	*Scenario 4*	*Scenario 5*	*Scenario 6*
Simulation length (h)		1 176					
V_{tank} (m^3)		55 300					
$Renewal_{tank}$ (day^{-1})		0.05					
$Phyto_{GrowthRate}$ (day^{-1})		0.4					
$TotalStock_{weight}$ (kg)		1 000				3 000	
Distribution per grade (%)	T4	30					
	T6	50					
	T8	20					
MortalityRate (% yr^{-1})	T4	30					
	T6	20					
	T8	10					
T (˚C)		15	25	30	20	20	20
S (psu)		36					
$C_{tank\_initial}$ (cells μL^{-1})		150	150	100	180	180	100
C_{in} (cells μL^{-1})		1					

All the simulations were run considering the system working on with the south system (SS), where the production tank volume (V_{tank}) is about 55 300 m^3. The renewal rate ($Renewal_{tank}$) was set as 0.05 day^{-1}, the phytoplankton growth rate ($Phyto_{GrowthRate}$) as 0.4 day^{-1} and the external phytoplankton concentration (C_{in}) as 1 cells μL^{-1}, within the previously described ranges. Size class mortality rates were assumed to be 30, 20 and 10% (T4, T6, and T8 respectively).

5.2.2. Outputs of the dynamic model application

5.2.2.1. Overview

Simulations of the oyster spat individual weight show a similar pattern for all the scenarios as well as for all the size classes. Predictions show an exponential growth in the first two weeks, being the maximum weight achieved between the end of week 2 and the beginning of week 3, followed by a decrease in individual weight until the end of the simulations. This trend is directly influenced by the availability of food inside the tank. In all the scenarios the food concentration reaches its maximum value before the first two weeks, being that by the end of week 2 is practically zero, remaining in this state until the end of the simulation period. Such behavior has often been observed in Bivalvia's nursery (François Hubert, Bivalvia, personal communication), which indicates a proximity between simulated and observed food concentration. Despite this, it should be remembered that the model only translates the food as phytoplankton when this can be composed of other forms not included in the model (e.g. detritus, Machás et al., 2003; Duarte et al., 2008).

A comparison between scenarios 1, 2, 3 and 4 (Figure 5.2 to Figure 5.5) shows that simulations for scenario 3 are the one that reached the maximum individual weights during the simulation period, while the higher final individual weights were reached for scenario 1. As expected, simulations for scenarios 5 and 6 (Figure 5.6 and Figure 5.7) show lower growths in relation to the other scenarios, due to the initial stock weight being 3 times higher.

Simulated final stock weights reached considerably higher values for scenarios 1, 2, 3 and 4 in comparison with scenarios 5 and 6 (Table 5.6).

5.2.2.2. Individual weight and tank concentrations

For scenario 1 the model simulations (Figure 5.2) show maximum individual weights of about 4.7, 6.1 and 9.5 g TFW ind^{-1} (for batches T4, T6, and T8 respectively), reached at the end of week 2. Final individual weights are of about 2.8, 3.8 and 6.0 g TFW ind^{-1} (for batches T4, T6, and T8 respectively), around 40% lower in comparison with maximum simulated weights. The

concentration inside the tank reached its peak (around 539 cells μL^{-1}) at the end of week 1, being that by the end of week 2 the simulation shows a food depletion.

Model simulations of scenario 2 (Figure 5.3) show very similar results in relation to scenario 1. Maximum individual weights, reached by the end of week 2, are of about 4.9, 6.5 and 9.8 g TFW ind^{-1} (for batches T4, T6 and T8 respectively). Final individual weights are of about 1.9, 2.6 and 4.3 g TFW ind^{-1} (for batches T4, T6, and T8 respectively), around 60% lower in comparison with maximum simulated weights. The peak of food inside the tank (around 623 cells μL^{-1}) was also reached at the end of week 1, and a depletion was simulated by the end of week 2.

The obtained results for scenario 1 and 2 show that, for the considered system and stock conditions, temperature at 15˚C and 25˚C (scenario 1 and scenario 2 respectively) reproduce similar behaviors in the oyster spat growth. Despite simulated maximum individual weights in scenario 2 be slightly higher in relation to those simulated in scenario 1, the final weights are lower. This is due to: (i) lower clearance rates at 25˚C, which is translated into a lower food consumption, allowing a higher growth of phytoplankton in the first weeks and thus the reach of higher maximum individual weights; and (ii) higher standard metabolic rates at 25˚C, which have a more severe influence in the weight loss in comparison with standard metabolic rates at 15˚C, during the period in which the food is not enough to meet the metabolic expenditures (from the beginning of week 2 to the end of week 7).

Model simulations for scenario 3 (Figure 5.4) show the occurrence of maximum individual weights in the beginning of week 3, of about 7.3, 9.2 and 13.5 g TFW ind^{-1} (for batches T4, T6, and T8 respectively). Final simulated individual weights are of about 2.4, 3.3 and 5.2 g TFW ind^{-1} (for batches T4, T6, and T8 respectively), around 65% lower in relation to maximum individual weights. The simulated food concentration shows a peak (around 981 cells μL^{-1}) in the beginning of week 2, and a depletion of food by the middle of week 3.

For scenario 4 the model simulations (Figure 5.5) show maximum individual weights of about 4.5, 5.9 and 9.1 g TFW (for batches T4, T6 and T8 respectively), reached by the end of week 2. Final individual weights are of about 2.1, 2.9 and 4.8 g TFW ind^{-1} (for batches T4, T6, and T8 respectively), around 50% lower in comparison with simulated maximum individual weights. The food concentration shows its maximum value (around 540 cells μL^{-1}) by the end of week 1, and by the end of week 2, the simulation shows a depletion of food.

Even with a higher initial food concentration considered in scenario 4, the achieved peak of food concentration is lower in comparison with the peak simulated for scenario 3. This behavior is

linked with: (i) higher initial food concentrations and (ii) higher clearance rates (temperature set at 20˚C), which translates into higher individual weights by the end of week 1. In turn, this increment in weight has a positive influence in the increase of individual clearance rates, impeding the reaching of higher concentrations.

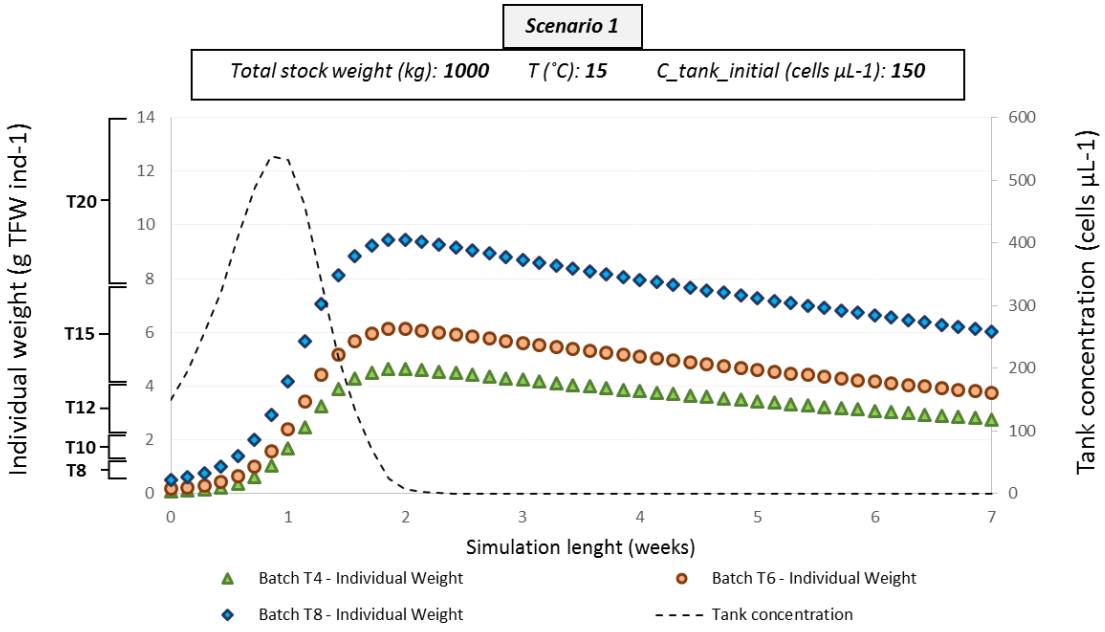

Figure 5.2 – Simulations of *Crassostrea gigas* spat individual growth and tank concentration for Scenario 1. The individuals are classified by batch according to the initial weight (T4, T6, T8).

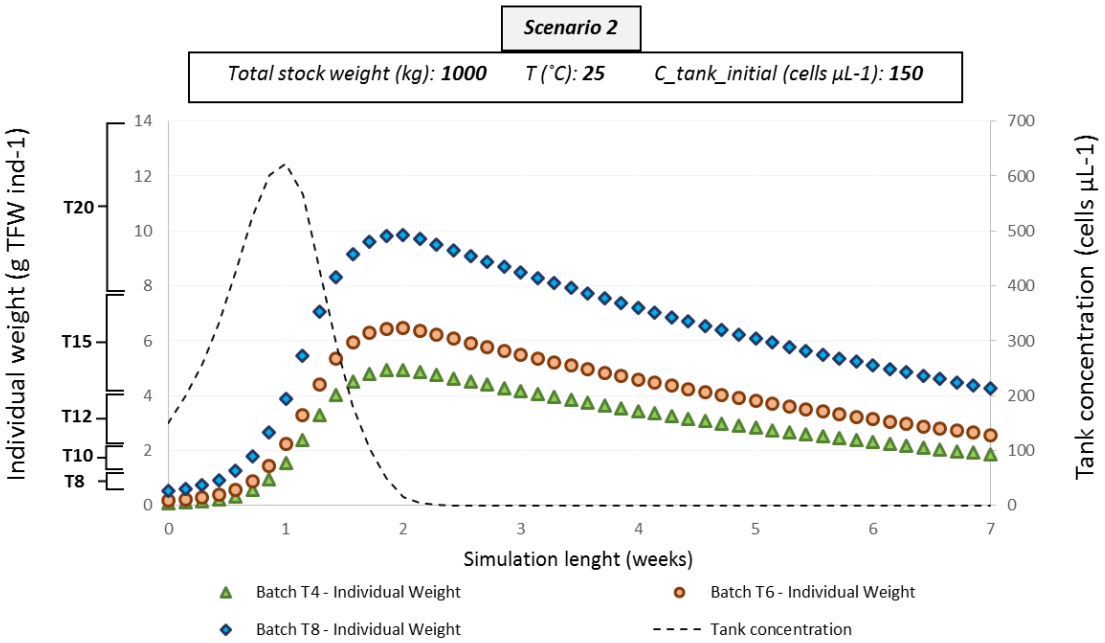

Figure 5.3 – Simulations of *Crassostrea gigas* spat individual growth and tank concentration for Scenario 2. The individuals are classified by batch according to the initial weight (T4, T6, T8).

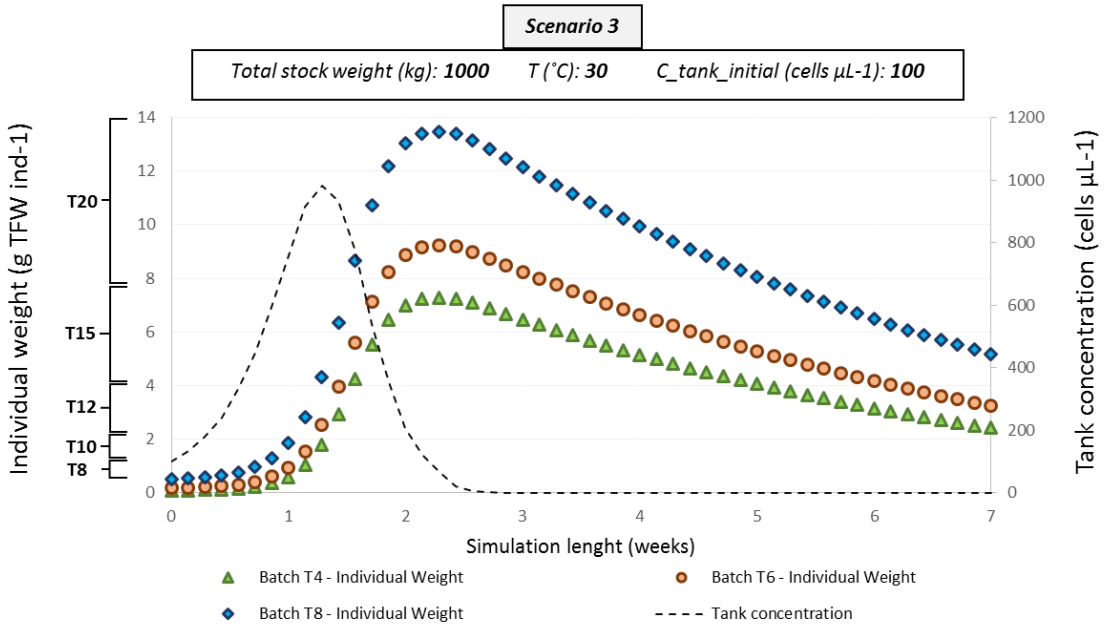

Figure 5.4 – Simulations of *Crassostrea gigas* spat individual growth and tank concentration for Scenario 3. The individuals are classified by batch according to the initial weight (T4, T6, T8).

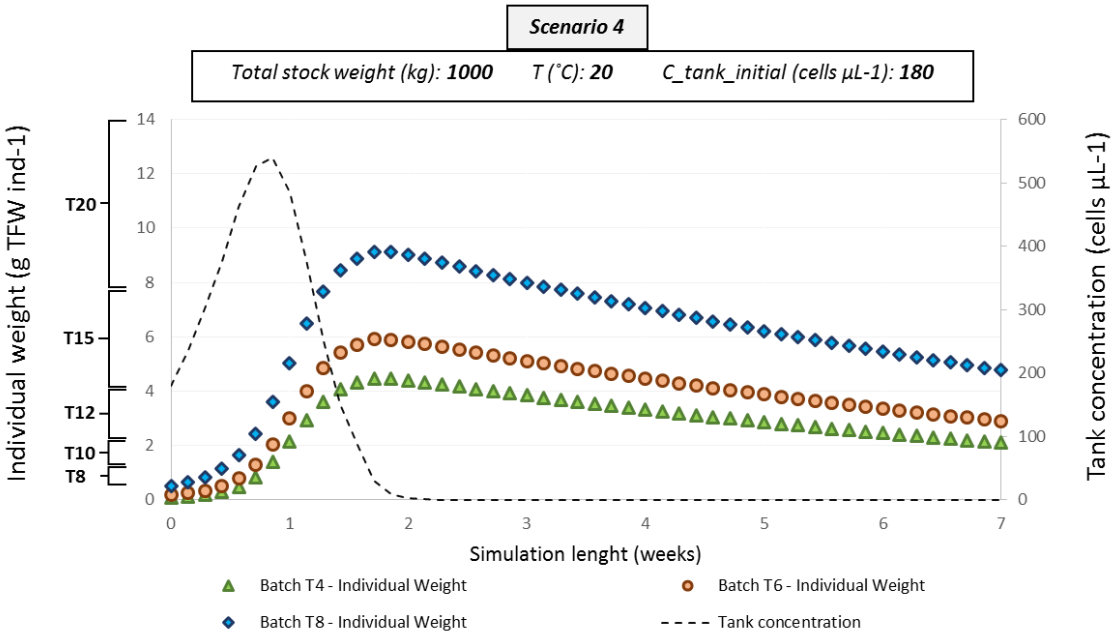

Figure 5.5 – Simulations of *Crassostrea gigas* spat individual growth and tank concentration for Scenario 4. The individuals are classified by batch according to the initial weight (T4, T6, T8).

Model simulations for scenario 5 and 6 show lower individual weight values, due to initial stock be larger in comparison with the other scenarios.

For scenario 5 the model simulations (Figure 5.6) show maximum individual weights of about 0.7, 1.0 and 2.0 g TFW ind^{-1} (for batches T4, T6, and T8 respectively), reached by the middle of week 2. Final individual weights are of about 0.2, 0.4 and 0.8 g TFW ind^{-1} (for batches T4, T6, and T8 respectively), around 65% lower in comparison with maximum simulated weights. The concentration inside the tank reached its peak (around 219 cells μL^{-1}) by the middle of week 1, being that by the middle of week 2 the simulation shows a food depletion.

Model simulations for scenario 6 (Figure 5.7) show the occurrence of maximum individual weights in the middle of week 2, of about 0.5, 0.8 and 1.7 g TFW ind^{-1} (for batches T4, T6, and T8 respectively). Final simulated individual weights are of about 0.2, 0.3 and 0.7 g TFW ind^{-1} (for batches T4, T6, and T8 respectively), around 65% lower in relation to maximum individual weights. The simulated food concentration shows a peak (around 153 cells μL^{-1}) in the middle of week 1, and a depletion of food by the middle of week 2.

Comparing scenarios 5 and 6 with the other scenarios it is possible to identify that high initial stocks do not enable the reaching of higher phytoplankton concentrations, due to higher food consumptions, thus translating into lower growths.

Nevertheless, it is important to highlight that during all the simulations it was considered a constant phytoplankton growth rate, which may not be the best way to represent the growth of phytoplankton inside the tank. For example, if nutrient limitation occurs at some point, which is unknown, the growth dynamics of phytoplankton may change and thus affect oyster growth.

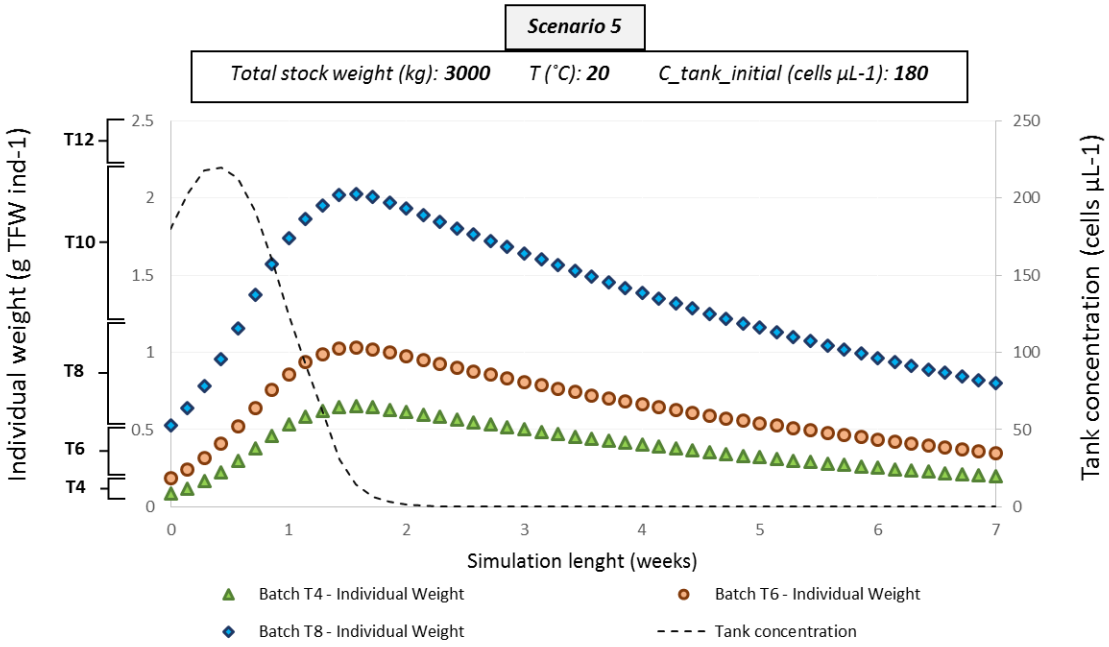

Figure 5.6 – Simulations of *Crassostrea gigas* spat individual growth and tank concentration for Scenario 5. The individuals are classified by batch according to the initial weight (T4, T6, T8).

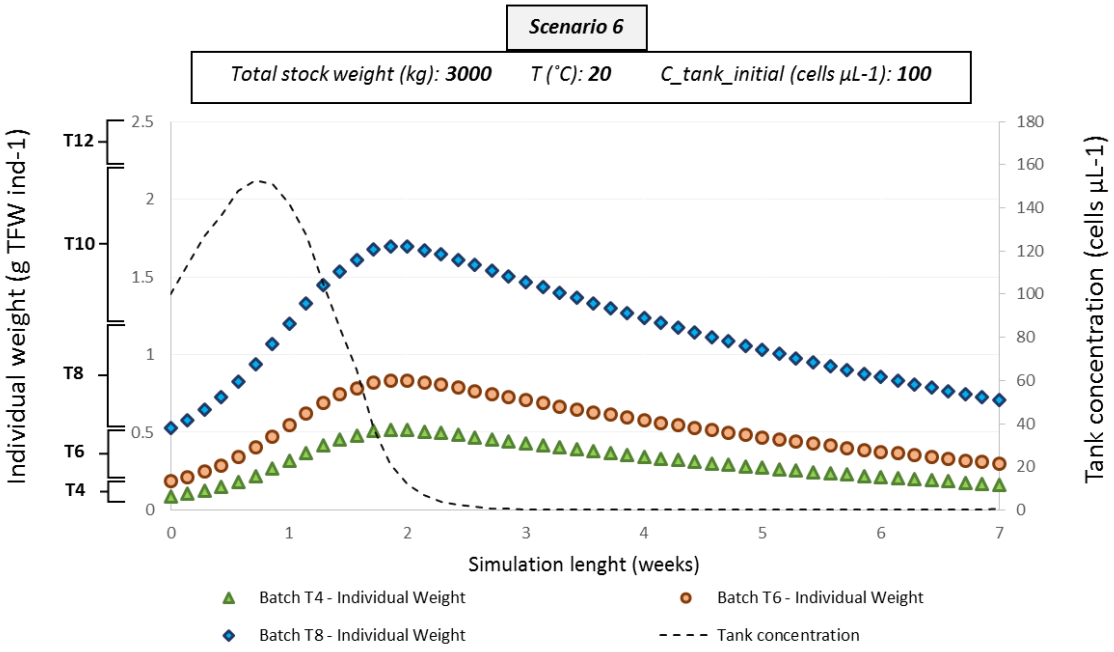

Figure 5.7 – Simulations of *Crassostrea gigas* spat individual growth and tank concentration for Scenario 6. The individuals are classified by batch according to the initial weight (T4, T6, T8).

5.2.2.3. Final stock weight

Simulated final stocks show big differences in weight when it is considered low or high initial stock weights (1 000 and 3 000 kg respectively, Table 5.6). Scenarios 1, 2, 3 and 4 (low initial stock weight) show final stock weights from 14 500 kg up to around 21 000 kg, distributed by size class T8 or by superior size classes. Scenarios 5 and 6 (high initial stock weight) show final stock weights around 5 000 kg, distributed by T6, T8 or by superior size classes in scenario 5, and by the T4, T6, T8 or superior size classes in scenario 6.

Table 5.5 – Final stock weight for each scenario, divided by size classes, and the relation between initial and final stock weight.

	Final stock weight (kg)				**Stock weight increase relative to initial stock (%)**
	By size class			Total stock	
	T4	T6	≥ T8		
Scenario 1	0	0	21 290	21 290	2 029
Scenario 2	0	0	14 518	14 518	1 352
Scenario 3	0	0	18 519	18 519	1 752
Scenario 4	0	0	16 358	16 358	1 536
Scenario 5	0	4 716	903	5 079	70
Scenario 6	1 623	2 363	796	4 782	60

The final stock weight from scenarios 1, 2, 3 and 4 show increases in relation to the initial stock weight from 1 300 up to 2 000 %, while scenarios 5 and 6 show substantially smaller increases (60 and 70 %). This is a very interesting finding, which for the model assumptions, system conditions, and the considered stock distribution, allows to state that lower initial stock weights are preferable for reaching higher final stock weights.

It is important to highlight that the highest stock weights for each scenario were achieved at the time which the maximum individual weights were reached. So, if a part of the stock was harvested at that time, a different final stock weight would be observed, in which final individual weights probably would be higher in relation to those presented in the previous sub-section 5.2.2.2.

5.3. General discussion on the application of the models

The application of the two modelling approaches presented in this work, in Bivalvia's commercial nursery, was carried out for hypothetical scenarios, with the objective of guiding the management towards production optimization.

As a first approach, a static mass balance model for oyster nurseries (presented in section 3) was used to estimate the maximum stocks sustained within a given feeding range. Maximum stocks were estimated based on the definition of hypothetical scenarios and stock distributions, resulting in stock estimates from around 22×10^6 to around 490×10^6 individuals. However, these high stock estimates, highly variable, seems to be unrealistic for Bivalvia's system, which can be mainly explained by:

(i) Consideration of a high range of phytoplankton growth rates, in all the scenarios defined. Inside Bivalvia's production tank the main source of phytoplankton seems to be the growth itself. Therefore, the definition of a big difference between the boundaries of this range is translated into a high variability of the stocks estimates. Should be noted that the assumed values of the phytoplankton growth rates were based on experiments of the community net primary productions of the Ria Formosa, run for different nutrient concentrations (Domingues et al., 2015), and it is most likely that these values are not in agreement with the nutrient availability in Bivalvia's production tank. Before entering in operation, a phytoplankton blooming ponds takes about a month and a half to be filled in completely, at the same time that enriches its phytoplankton concentration, which may lead to a nutrient limitation by the time it is operating.

(ii) Assumption of total mix of the water inside the phytoplankton blooming ponds. This assumption leaded to the consideration of the total volume of Bivalvia's production tank in all scenarios defined. However, in case there are "dead zones", the volume to consider should be lower in relation to total volume, which will result in lower stock estimates.

Taking these two points into account, future applications of this model in Bivalvia's nursery should be done considering lower phytoplankton growth rates (e.g. it is suggested the assumption of 0.1 – 0.4 day^{-1}, for low and high growth respectively), and a smaller tank volume (e.g. if there are suspicions of 50% of "dead zones", the volume to consider should be 36 300 and 28 300 m^3, for operation with NS and SS respectively). Nevertheless, it cannot be considered that these values are really representative, since they are only assumptions. Estimating the

values of this parameters through field assessments (e.g. by the use of an ADCP, for hydrodynamics assessment; and nutrient and light intensity surveys, to later estimate the phytoplankton growth rates) would reduce the associated uncertainty, and thus would be an asset for a better application of this model.

Other factors that contributed to the variability of the estimated stocks were the water temperature and stock distribution. As explained before (see sub-section 4.1.2.3), water temperature has effects on clearance rate, being its maximum value achieved at 19˚C. Thus, the closer the water temperature is to this value, the lower the stock estimates, and vice-versa (see sub-section 4.1.2.3 and Figure 5.1). In what concerns the stock distribution, as bigger individuals present higher individual clearance rates, a stock constituted by bigger individuals will filter out more food than a stock constituted by smaller individuals (assuming the same number of individuals per stock). This means that maximum stocks estimates (expressed as number of individuals) for stock distributions mainly constituted by bigger individuals (e.g. from size class T8) will be lower in relation to estimates for stocks distributions constituted by smaller individuals (e.g. from size class T3).

As a second approach, for simulations of oyster spat individual growth, food availability within the farming system and stock biomass over time, a dynamic model for oyster nurseries was herein developed and applied to hypothetical scenarios in Bivalvia's nursery. Due to the lack of historical data, a model validation and calibration was not carried out for this system, thus bringing uncertainty to the model outputs of this application. Besides, in the scenario definition, it was also considered a phytoplankton growth rate and a tank volume that may not represent truly the reality, as pointed out previously. However, by dismissing the magnitude of the simulated values, it was possible to withdrawn the very interesting finding that a low initial stock weight are preferable for reaching a high stock weight. This is related to the fact that a larger initial stock filters out more food, thus not allowing the reaching of higher phytoplankton concentrations by preventing its growth, which will consequently limit the oyster growth.

Moreover, the application of this model in Bivalvia's nursery have shown that for both high and low stocks, around two weeks after a phytoplankton blooming pond be connected to the tank of the FLUPSY occurs a full depletion of food. This behavior has often been observed in Bivalvia's nursery, which brings a little bit more confidence about the model predictions. Future applications of this model can be done to assess if there is any stock (lower comparable to the currently practicable in Bivalvia's nursery) that would prevent this depletion.

Since one of the most important factors related with the Bivalvia's production is the phytoplankton growth, in order to encompass all the dynamics associated with it, it would be interesting in the future to couple a primary production model to the dynamic model for oyster nurseries. This model do not should only consider the inflow of nutrients from the water renewal, but also the mineralization of nutrients from the sediments, which actually could be the major source of nutrients in Bivalvia's nursery.

6. Conclusions

The main of objectives of this work were: (i) the development and validation of two models to be used as tools to support the management of oyster commercial nurseries; and (ii) application of both models in a commercial nursery, aiming at guide the management towards production optimization.

Each model is based on a different approach, to account with different levels of input data. First, it is presented a static mass balance model for oyster nurseries (section 3), which requires a lower level of input data, but which in turn provides limited output data. In second, it is presented a dynamic oyster model for nurseries (section 4), which requires a higher level of input data, thus providing a wider range of output data.

Both models were validated for datasets from the scientific literature, showing good agreements between the simulated and observed data. However, should be highlighted, that prior to the application of these models for a given system, a model validation and calibration must be carried out in order to increase the accuracy of model outputs, and thus the confidence in its results. For instance, the sensitivity analysis of the dynamic oyster model for nurseries (see sub-section 4.6) showed changes up to 61% in the simulated oyster biomass, by changing the model parameters in 10%. This means that an incorrect calibration of these parameters, for a given system, will be translated in highly inaccurate results. Moreover, part of the high sensitivity of the model may be related to the fact of some processes (e.g. ingestion and assimilation) have been modeled as constant fractions, when these are known to be variable. Thus, future developments should be made to account for a better definition of those processes, for which non-phytoplankton particles (i.e. detritus and inorganic matter) must also be included in the model formulation.

Due to a lack of data to properly validate, calibrate and run the models, the application of both models, in Bivalvia's nursery, was performed for hypothetical scenarios. Even though, some useful insights for production optimization were withdrawn from those applications:

- Low initial stocks are preferable for reaching high final stocks.
- Water temperature at 19˚C is the one that allows to sustain lower stocks (corresponding to March, April and October).

As the outputs from the static mass balance model application seems to be overestimated, it is not possible to assume with confidence the maximum stock to hold in Bivalvia's nursery. Regarding this, new scenarios must be defined, by considering lower phytoplankton growth

rates, as well as lower tank volumes, for suspicions of “dead zones” related with the water mix inside the phytoplankton blooming ponds (see sub-section 5.3). The same applies for future applications of the dynamic oyster model for nurseries.

In what concerns the simulations of oyster growth and stock biomass, from the application of the dynamic model for oyster nurseries, these also appear to be slightly overestimated. However, the simulated behavior of food concentration inside the tank is in agreement with the reported by Bivalvia’s nursery managers. This highlights the need to validate and calibrate the model in this system, in order to have a higher level of confidence in the outputs. In addition, since one of the most important factors related with the Bivalvia’s production is the phytoplankton growth, further developments should consider the coupling of a primary production model to the dynamic model for oyster nurseries (see sub-section 5.3).

Assessments aiming at the identification of key-factors for production optimization, can be carried out by complementing these two models, especially for the cases where there is lacking some representativeness of the input data. For instance, envelope estimates of maximum stocks can be obtained by applying the static mass balance model. After this application, a set of stocks within the estimated range can be defined, and the dynamic model applied for each one. This way, it could be compared the dynamic of food availability and oyster growth between several stocks, in order to choose the one that best suit to optimize the production.

References

Alunno-Bruscia, M., Bourlès, Y., Maurer, D., Robert, S., Mazurié, J., Gangnery, A., ... & Pouvreau, S. (2011). A single bio-energetics growth and reproduction model for the oyster *Crassostrea gigas* in six Atlantic ecosystems. *Journal of sea research*, *66*(4), 340-348.

Bacher, C., & Baud, J. P. (1992). Intensive rearing of juvenile oysters *Crassostrea gigas* in an upwelling system: optimization of biological production. *Aquatic Living Resources*, *5*(2), 89-98.

Bacher, C., & Gangnery, A. (2006). Use of dynamic energy budget and individual based models to simulate the dynamics of cultivated oyster populations. *Journal of Sea Research*, *56*(2), 140-155.

Baker, S., K. Grogan, S. Larkin, L. Sturmer. (2015). "Green" Clams: Estimating the Value of Environmental Benefits (Ecosystem Services) Generated by the Hard Clam Aquaculture Industry in Florida. Project report. University of Florida IFAS research and extension faculty. Pp 10. Available at: http://shellfish.ifas.ufl.edu/wp-content/uploads/environmental-benefits.pdf

Barbosa, A. B. (2010). Seasonal and interannual variability of planktonic microbes in a mesotidal coastal lagoon (Ria Formosa, SE Portugal): impact of climatic changes and local human influences. *Coastal Lagoons: critical habitats of environmental change*, 335-366.

Barillé, L., Prou, J., Héral, M., & Bourgrier, S. (1993). No influence of food quality, but ration-dependent retention efficiencies in the Japanese oyster *Crassostrea gigas*. *Journal of experimental marine Biology and Ecology*, *171*(1), 91-106.

Barillé, L., Prou, J., Héral, M., & Razet, D. (1997). Effects of high natural seston concentrations on the feeding, selection, and absorption of the oyster *Crassostrea gigas* (Thunberg). *Journal of experimental marine biology and ecology*, *212*(2), 149-172.

Barrett E.M. (1963). The California oyster industry. 103 pp. Fish bulletin, 123. State of California, Department of Fish and Game. Available at: http://content.cdlib.org/view?docId=kt629004n3;NAAN=13030&chunk.id=d0e272&toc.id=d0e269&toc.depth=1&brand=calisphere&anchor.id=tab3

Bayne, B. L. (1999). Physiological components of growth differences between individual oysters (*Crassostrea gigas*) and a comparison with *Saccostrea commercialis*. *Physiological and biochemical zoology*, *72*(6), 705-713.

Bayne, B. L. (2009). Carbon and nitrogen relationships in the feeding and growth of the Pacific oyster, *Crassostrea gigas* (Thunberg). *Journal of Experimental Marine Biology and Ecology*, *374*(1), 19-30.

Bayne, B. L. (2017). *Biology of Oysters*. London, U.K: Academic Press.

Beninger, P. G., Valdizan, A., Decottignies, P., & Cognie, B. (2008). Impact of seston characteristics on qualitative particle selection sites and efficiencies in the pseudolamellibranch bivalve *Crassostrea gigas*. *Journal of Experimental Marine Biology and Ecology*, *360*(1), 9-14.

Bougrier, S., Geairon, P., Deslous-Paoli, J. M., Bacher, C., & Jonquières, G. (1995). Allometric relationships and effects of temperature on clearance and oxygen consumption rates of *Crassostrea gigas* (Thunberg). *Aquaculture*, *134*(1), 143-154.

Bourlés, Y., Alunno-Bruscia, M., Pouvreau, S., Tollu, G., Leguay, D., Arnaud, C., ... & Kooijman, S. A. L. M. (2009). Modelling growth and reproduction of the Pacific oyster *Crassostrea gigas*: advances in the oyster-DEB model through application to a coastal pond. *Journal of Sea Research*, *62*(2), 62-71.

Breese W.P. & R.E. Malouf. (1975). Hatchery Manual for the Pacific Oyster. Oregon State University, Sea Grant College Program. Agricultural Experiment Station. Publication no. ORESU-H-75-002. Special Report No. 443. Available at: http://ir.library.oregonstate.edu/xmlui/bitstream/handle/1957/6637/?sequence=1

Brown, M. R., McCausland, M. A., & Kowalski, K. (1998). The nutritional value of four Australian microalgal strains fed to Pacific oyster *Crassostrea gigas* spat. *Aquaculture*, *165*(3), 281-293.

Byron, C.J. & B.A. Costa-Pierce. (2013). Carrying capacity tools for use in the implementation of an ecosystems approach to aquaculture. In: L.G. Ross, T.C. Telfer, L. Falconer, D. Soto & J. Aguilar-Manjarrez, editors. Site selection and carrying capacities for inland and coastal aquaculture, pp. 87–101. FAO/Institute of Aquaculture, University of Stirling, Expert Workshop, 6–8 December 2010. Stirling, the United Kingdom of Great Britain and Northern Ireland. FAO Fisheries and Aquaculture Proceedings No. 21. Rome, FAO. 282 pp.

Ceia, F. R., Patrício, J., Marques, J. C., & Dias, J. A. (2010). Coastal vulnerability in barrier islands: The high risk areas of the Ria Formosa (Portugal) system. *Ocean & Coastal Management*, *53*(8), 478-486.

Cerco, C. F., & Noel, M. R. (2007). Can oyster restoration reverse cultural eutrophication in Chesapeake Bay? *Estuaries and Coasts*, *30*(2), 331-343. doi: 10.1007/BF02700175

Chapra, S.C. (Ed.). (1997). *Surface Water–Quality Modelling*.New York, NY: McGraw-Hill Inc.

Claus, C., Maeckelberghe, H., & de Pauw, N. (1983). Onshore nursery rearing of bivalve molluscs in Belgium. *Aquacultural Engineering*, *2*(1), 13-26.

Coen, L. D., Dumbauld, B. R. and Judge, M. L. (2011) Expanding Shellfish Aquaculture: A Review of the Ecological Services Provided by and Impacts of Native and Cultured Bivalves in Shellfish-Dominated Ecosystems, in Shellfish Aquaculture and the Environment (ed S. E. Shumway), Wiley-Blackwell, Oxford, UK. doi: 10.1002/9780470960967.ch9

Cranford, P. J., Ward, J. E., & Shumway, S. E. (2011). Bivalve filter feeding: Variability and limits of the aquaculture biofilter. In S. E. Shumway (Ed.), *Shellfish aquaculture and the environment* (pp. 81–124). Chichester, UK: John Wiley & Sons Inc.

Crawford, C. M., Macleod, C. K., & Mitchell, I. M. (2003). Effects of shellfish farming on the benthic environment. *Aquaculture*, *224*(1), 117-140.

Cummins, K.W. and Wuycheck, J.C., (1971). Caloric equivalents for investigations in ecological energetics. Int. Ver. Theor. Angew. Limnol., 18: 1-158.

DePiper, G. S., Lipton, D. W., & Lipcius, R. N. (2017). Valuing Ecosystem Services: Oysters, Denitrification, and Nutrient Trading Programs. *Marine Resource Economics*, *32*(1), 1-20. doi: 10.1086/688976

Deslous-Paoli, J. M., & Héral, M. (1988). Biochemical composition and energy value of *Crassostrea gigas* (Thunberg) cultured in the bay of Marennes-Oléron. *Aquatic Living Resources*, *1*(4), 239-249.

Dewey, W., Davis, J. P., & Cheney, D. C. (2011). Shellfish aquaculture and the environment: An industry perspective. *Shellfish aquaculture and the environment*.

Doiron, S. (2008). Reference Manual for Oyster Aquaculturists. *New Brunswick Department of Agriculture, Fisheries and Aquaculture*.

Domingues, R. B., Guerra, C. C., Barbosa, A. B., & Galvão, H. M. (2015). Are nutrients and light limiting summer phytoplankton in a temperate coastal lagoon?. *Aquatic Ecology*, *49*(2), 127-146.

Duarte, P., Azevedo, B., Ribeiro, C., Pereira, A., Falcão, M., Serpa, D., ... & Reia, J. (2008). Scenario Analysis in Ria Formosa with EcoDynamo.

Duarte, P., Meneses, R., Hawkins, A. J. S., Zhu, M., Fang, J., & Grant, J. (2003). Mathematical modelling to assess the carrying capacity for multi-species culture within coastal waters. *Ecological Modelling*, *168*(1), 109-143.

Dumbauld, B. R., Ruesink, J. L., & Rumrill, S. S. (2009). The ecological role of bivalve shellfish aquaculture in the estuarine environment: A review with application to oyster and clam culture in West Coast (USA) estuaries. *Aquaculture*, *290*(3), 196-223.

Dumbauld, B. R., Ruesink, J. L., & Rumrill, S. S. (2009). The ecological role of bivalve shellfish aquaculture in the estuarine environment: A review with application to oyster and clam culture in West Coast (USA) estuaries. *Aquaculture*, *290*(3), 196-223.

Fábregas, J., Herrero, C., Cabezas, B., & Abalde, J. (1985). Mass culture and biochemical variability of the marine microalga *Tetraselmis suecica* Kylin (Butch) with high nutrient concentrations. Aquaculture, 49(3-4), 231-244.

FAO. (2017a). Fishery and Aquaculture Statistics. Global aquaculture production 1950-2015 (FishstatJ). In: FAO Fisheries and Aquaculture Department [online]. Rome. Updated 2017. www.fao.org/fishery/statistics/software/fishstatj/en

FAO. (2017b).The future of food and agriculture – Trends and challenges. Rome.

Ferreira, J. G., & Bricker, S. B. (2016). Goods and services of extensive aquaculture: shellfish culture and nutrient trading. *Aquaculture International*, *24*(3), 803-825.

Ferreira, J. G., Hawkins, A. J. S. and Bricker, S. B. (2011) The Role of Shellfish Farms in Provision of Ecosystem Goods and Services, in Shellfish Aquaculture and the Environment (ed S. E. Shumway), Wiley-Blackwell, Oxford, UK. doi: 10.1002/9780470960967.ch1

Ferreira, J. G., Hawkins, A. J. S., & Bricker, S. B. (2007). Management of productivity, environmental effects and profitability of shellfish aquaculture—the Farm Aquaculture Resource Management (FARM) model. *Aquaculture*, *264*(1), 160-174.

Ferreira, J. G., Saurel, C., & Ferreira, J. M. (2012). Cultivation of gilthead bream in monoculture and integrated multi-trophic aquaculture. Analysis of production and environmental effects by means of the FARM model. *Aquaculture*, *358*, 23-34.

Ferreira, J. G., Saurel, C., e Silva, J. L., Nunes, J. P., & Vazquez, F. (2014). Modelling of interactions between inshore and offshore aquaculture. *Aquaculture*, *426*, 154-164.

Ferreira, J. G., Saurel, C., Nunes, J. P., Ramos, L., Lencart e Silva, J. D., Vazquez, F., ... Rocha, M. (2013). FORWARD - Framework for Ria Formosa Water Quality, Aquaculture, and Resource Development.

Filgueira, R., Byron, C. J., Comeau, L. A., Costa-Pierce, B., Cranford, P. J., Ferreira, J. G., ... & McKindsey, C. W. (2015a). An integrated ecosystem approach for assessing the potential role of cultivated bivalve shells as part of the carbon trading system. *Marine Ecology Progress Series*, *518*, 281-287.

Filgueira, R., L.A. Comeau, T. Guyondet, C.W. McKindsey & C.J. Byron. (2015b). *Modelling Carrying Capacity of Bivalve Aquaculture: A Review of Definitions and Methods.* In: R.A. Meyers,

editor. Encyclopedia of Sustainability Science and Technology. Springer New York. (pp. 1-33.) doi: 10.1007/978-1-4939-2493-6_945-1

Flimlin, G. (2000). Nursery and growout methods for aquacultured shellfish. *Northeastern Regional Aquaculture Center Publication No. NRAC 00-002*.

Forrest, B. M., Keeley, N. B., Hopkins, G. A., Webb, S. C., & Clement, D. M. (2009). Bivalve aquaculture in estuaries: review and synthesis of oyster cultivation effects. *Aquaculture*, *298*(1), 1-15.

Fortmann-Roe, S. (2014). Insight Maker: A general-purpose tool for web-based modelling & simulation. *Simulation Modelling Practice and Theory*, *47*, 28-45.

Gallardi, D. (2014). Effects of bivalve aquaculture on the environment and their possible mitigation: a review. *Fisheries and Aquaculture Journal*, *5*(3), 1. doi:10.4172/2150-3508.1000105

Gangnery, A., Bacher, C., & Buestel, D. (2001). Assessing the production and the impact of cultivated oysters in the Thau lagoon (Mediterranee, France) with a population dynamics model. *Canadian Journal of Fisheries and Aquatic Sciences*, *58*(5), 1012-1020. doi: 10.1139/f01-028

Gangnery, A., Bacher, C., & Buestel, D. (2004). Modelling oyster population dynamics in a Mediterranean coastal lagoon (Thau, France): sensitivity of marketable production to environmental conditions. *Aquaculture*, *230*(1), 323-347.

Gangnery, A., C. Bacher & D. Buestel. 2011. Assessing the production and the impact of cultivated oysters in the Thau lagoon (Mediterranee, France) with a population dynamics model. Canadian Journal of Fisheries and Aquatic Sciences 58:1012-1020. doi: 10.1139/f01-028

García-Esquivel, Z., Bricelj, V. M., & Felbeck, H. (2002). Metabolic depression and whole-body response to enforced starvation by *Crassostrea gigas* postlarvae. *Comparative Biochemistry and Physiology Part A: Molecular & Integrative Physiology*, *133*(1), 63-77.

Gerdes, D. (1983a). The Pacific oyster *Crassostrea gigas*: Part I. Feeding behaviour of larvae and adults. *Aquaculture*, *31*(2-4), 195-219.

Gerdes, D. (1983b). The Pacific oyster *Crassostrea gigas*: Part II. Oxygen consumption of larvae and adults. *Aquaculture*, *31*(2-4), 221-231.

Gnaiger, E. (1983). Calculation of energetic and biochemical equivalents of respiratory oxygen consumption. In *Polarographic oxygen sensors* (pp. 337-345). Springer Berlin Heidelberg.

Gosling, E. (2004). *Bivalve Molluscs: Biology, Ecology and Culture*. Oxford, United Kingdom: Blackwell Publishing

Goulletquer, P., Wolowicz, M., Latala, A., Geairon, P., Huvet, A., & Boudry, P. (1999). Comparative analysis of oxygen consumption rates between cupped oyster spat of *Crassostrea gigas* of French, Japanese, Spanish and Taiwanese origins. *Aquatic Living Resources*, *12*(4), 271-277.

Grangeré, K., Ménesguen, A., Lefebvre, S., Bacher, C., & Pouvreau, S. (2009). Modelling the influence of environmental factors on the physiological status of the Pacific oyster *Crassostrea gigas* in an estuarine embayment; The Baie des Veys (France). *Journal of Sea Research*, *62*(2), 147-158.

Grant, J., & Bacher, C. (1998). Comparative models of mussel bioenergetic and their validation at field culture sites. *Journal of Experimental Marine Biology and Ecology*, *219*(1), 21-44.

Grant, J., Curran, K. J., Guyondet, T. L., Tita, G., Bacher, C., Koutitonsky, V., & Dowd, M. (2007). A box model of carrying capacity for suspended mussel aquaculture in Lagune de la Grande-Entrée, Iles-de-la-Madeleine, Québec. *Ecological modelling*, *200*(1), 193-206.

Guyondet, T., Roy, S., Koutitonsky, V. G., Grant, J., & Tita, G. (2010). Integrating multiple spatial scales in the carrying capacity assessment of a coastal ecosystem for bivalve aquaculture. *Journal of Sea Research*, *64*(3), 341-359.

Halpern, B. S., Selkoe, K. A., Micheli, F., & Kappel, C. V. (2007). Evaluating and ranking the vulnerability of global marine ecosystems to anthropogenic threats. *Conservation Biology*, *21*(5), 1301-1315.

Hawkins, A. J. S., Bayne, B. L., Bougrier, S., Héral, M., Iglesias, J. I. P., Navarro, E., ... & Urrutia, M. B. (1998). Some general relationships in comparing the feeding physiology of suspension-feeding bivalve molluscs. *Journal of Experimental Marine Biology and Ecology*, *219*(1), 87-103.

Hawkins, A. J. S., Duarte, P., Fang, J. G., Pascoe, P. L., Zhang, J. H., Zhang, X. L., & Zhu, M. Y. (2002). A functional model of responsive suspension-feeding and growth in bivalve shellfish, configured and validated for the scallop *Chlamys farreri* during culture in China. *Journal of Experimental Marine Biology and Ecology*, *281*(1), 13-40.

Hawkins, A. J. S., Pascoe, P. L., Parry, H., Brinsley, M., Black, K. D., McGonigle, C., ... & O'Loan, B. (2013). Shellsim: A generic model of growth and environmental effects validated across contrasting habitats in bivalve shellfish. *Journal of Shellfish Research*, *32*(2), 237-253.

Helm, M.M. & N. Bourne. (2004). Hatchery culture of bivalves — a practical manual. *FAO Fisheries Technical* Paper 471. FAO, Rome. 178 pp.

Higgins, C. B., Stephenson, K., & Brown, B. L. (2011). Nutrient bioassimilation capacity of aquacultured oysters: quantification of an ecosystem service. *Journal of environmental quality*, *40*(1), 271-277.

Hitchcock, G. L. (1980). Diel variation in chlorophyll a, carbohydrate and protein content of the marine diatom *Skeletonema costatum*. Marine Biology, 57(4), 271-278.

Hyun, K. H., Pang, I. C., Klinck, J. M., Choi, K. S., Lee, J. B., Powell, E. N., ... & Bochenek, E. A. (2001). The effect of food composition on Pacific oyster *Crassostrea gigas* (Thunberg) growth in Korea: a modelling study. *Aquaculture*, *199*(1), 41-62.

Inglis, G., Hayden, B. J., & Ross, A. H. (2000). *An overview of factors affecting the carrying capacity of coastal embayments for mussel culture*. National Institute of Water & Atmospheric Research.

Ishiwata, Y., Ohi, N., Obata, M., & Taguchi, S. (2013). Carbon to volume relationship of *Isochrysis galbana* (Prymnesiophyceae) during cell divisions. *Plankton and Benthos Research*, *8*(4), 178-185.

Jiang, Z., Wang, G., Fang, J., & Mao, Y. (2013). Growth and food sources of Pacific oyster *Crassostrea gigas* integrated culture with Sea bass *Lateolabrax japonicus* in Ailian Bay, China. *Aquaculture international*, *21*(1), 45-52.

Jones, C., Branosky, E., Selman, M., & Perez, M. (2010). How nutrient trading could help restore the Chesapeake Bay. *World Resources Institute Working Paper*.

Jørgensen, S. E., & Bendoricchio, G. (2001). *Fundamentals of ecological modelling* (Vol. 21). Elsevier.

Kaiser, M. J., Laing, I., Utting, S. D., & Burnell, G. M. (1998). Environmental impacts of bivalve mariculture. *Journal of Shellfish research*, *17*(1), 59-66.

Kobayashi, M., Hofmann, E. E., Powell, E. N., Klinck, J. M., & Kusaka, K. (1997). A population dynamics model for the Japanese oyster, *Crassostrea gigas*. *Aquaculture*, *149*(3-4), 285-321.

Kobayashi, M., Msangi, S., Batka, M., Vannuccini, S., Dey, M. M., & Anderson, J. L. (2015). Fish to 2030: the role and opportunity for aquaculture. *Aquaculture economics & management*, *19*(3), 282-300.

Kooijman, S. A. L. M. (2000). *Dynamic energy and mass budgets in biological systems*. Cambridge university press.

Langton, R. W., & McKay, G. U. (1976). Growth of *Crassostrea gigas* (Thunberg) spat under different feeding regimes in a hatchery. *Aquaculture*, *7*(3), 225-233.

Liu, X., Duan, S., Li, A., Xu, N., Cai, Z., & Hu, Z. (2009). Effects of organic carbon sources on growth, photosynthesis, and respiration of *Phaeodactylum tricornutum*. Journal of Applied Phycology, 21(2), 239-246.

Loosanoff, V. L., & Tommers, F. D. (1948). Effect of suspended silt and other substances on rate of feeding of oysters. *Science*, *107*(2768), 69-70.

Lotze, H. K., Lenihan, H. S., Bourque, B. J., Bradbury, R. H., Cooke, R. G., Kay, M. C., ... & Jackson, J. B. (2006). Depletion, degradation, and recovery potential of estuaries and coastal seas. *Science*, *312*(5781), 1806-1809.

Machás, R., Santos, R., & Peterson, B. (2003). Tracing the flow of organic matter from primary producers to filter feeders in Ria Formosa lagoon, southern Portugal. *Estuaries and Coasts*, *26*(4), 846-856.

Majkowski, J. A. C. E. K. (1982). Usefulness and applicability of sensitivity analysis in a multispecies approach to fisheries management. In *Theory and management of tropical fisheries. ICLARM Conf. Proc. 9* (Vol. 360, pp. 149-165).

Mann, R., Burreson, E. M., & Baker, P. K. (1994). The Decline of the Virginia Oyster Fishery in Chesapeake Bay: Considerations for Introduction of a Non-Endemic Species, *Crassostrea gigas* (Thunberg, 1793)'. *Molluscan Introductions and Transfers: Risks Considerations and Implications*, *94*(2), 25.

McKindsey, C. W., Thetmeyer, H., Landry, T., & Silvert, W. (2006). Review of recent carrying capacity models for bivalve culture and recommendations for research and management. *Aquaculture*, *261*(2), 451-462.

Méléder, V., Barillé-Boyer, A. L., Baud, J. P., Barillé, L., Cognie, B., & Rosa, P. (2001). Modélisation de l'affinage de l'huître *Crassostrea gigas* alimentée avec la diatomée *Skeletonema costatum*. *Aquatic Living Resources*, *14*(1), 49-64.

Meseck, S. L., Li, Y., Dixon, M. S., Rivara, K., Wikfors, G. H., & Luther III, G. (2012). Effects of a commercial, suspended eastern oyster nursery upon nutrient and sediment chemistry in a temperate, coastal embayment. *Aquaculture Environment Interactions*, *3*(1), 65-79.

Montagnes, D. J., Berges, J. A., Harrison, P. J., & Taylor, F. (1994). Estimating carbon, nitrogen, protein, and chlorophyll a from volume in marine phytoplankton. Limnology and Oceanography, 39(5), 1044-1060.

Msangi, S., Kobayashi, M., Batka, M., Vannuccini, S., Dey, M. M., & Anderson, J. L. (2013). Fish to 2030: prospects for fisheries and aquaculture. *World Bank Report*, (83177-GLB), 102.

Neves, R. J. (1988). Flow process modelling in a salt marsh.

Newell, R. I., & Jordan, S. J. (1983). Preferential ingestion of organic material by the American oyster *Crassostrea virginica*. *Marine Ecology Progress Series*, 47-53.

Newell, R. I., & Mann, R. (2012). Shellfish aquaculture: ecosystem effects, benthic-pelagic coupling and potential for nutrient trading. *A Report Prepared for the Secretary of Natural Resources, Commonwealth of Virginia*.

Newton, A., & Mudge, S. M. (2003). Temperature and salinity regimes in a shallow, mesotidal lagoon, the Ria Formosa, Portugal. *Estuarine, Coastal and Shelf Science*, *57*(1), 73-85.

Nobre, A. M., Bricker, S. B., Ferreira, J. G., Yan, X., De Wit, M., & Nunes, J. P. (2011). Integrated environmental modelling and assessment of coastal ecosystems: application for aquaculture management. *Coastal Management*, *39*(5), 536-555. doi :10.1080/08920753.2011.600238

Nobre, A. M., Valente, L. M. P., & Neori, A. (2017). A nitrogen budget model with a user-friendly interface, to assess water renewal rates and nitrogen limitation in commercial seaweed farms. *Journal of Applied Phycology*, 1-17. doi: 10.1007/s10811-017-1164-9

Nobre, A.M., Soares, F., Ferreira, J.G. (accepted for publication). A mass balance model to assess food limitation in commercial oyster nurseries.

Nunes, J. P., Ferreira, J. G., Gazeau, F., Lencart-Silva, J., Zhang, X. L., Zhu, M. Y., & Fang, J. G. (2003). A model for sustainable management of shellfish polyculture in coastal bays. *Aquaculture*, *219*(1), 257-277.

Paltzat, D. L., Pearce, C. M., Barnes, P. A., & McKinley, R. S. (2008). Growth and production of California sea cucumbers (*Parastichopus californicus Stimpson*) co-cultured with suspended Pacific oysters (*Crassostrea gigas* Thunberg). *Aquaculture*, *275*(1), 124-137.

Pauly, D., & Zeller, D. (2017). Comments on FAOs State of World Fisheries and Aquaculture (SOFIA 2016). *Marine Policy*, *77*, 176-181.

Phatarpekar, P. V., Sreepada, R. A., Pednekar, C., & Achuthankutty, C. T. (2000). A comparative study on growth performance and biochemical composition of mixed culture of *Isochrysis galbana* and *Chaetoceros calcitrans* with monocultures. Aquaculture, 181(1), 141-155.

Platt, T., & Irwin, B. (1973). Caloric content of phytoplankton. *Limnology and Oceanography*, *18*(2), 306-310.

Pouvreau, S., Bourles, Y., Lefebvre, S., Gangnery, A., & Alunno-Bruscia, M. (2006). Application of a dynamic energy budget model to the Pacific oyster, *Crassostrea gigas*, reared under various environmental conditions. *Journal of Sea Research*, *56*(2), 156-167.

Quayle, D.B., (1988). Pacific oyster culture in British Columbia. *Canada Bulletin of Fisheries and Aquatic Science*, 218: 1-231.

Ren, J. S., & Ross, A. H. (2001). A dynamic energy budget model of the Pacific oyster *Crassostrea gigas*. *Ecological Modelling*, *142*(1), 105-120.

Ren, J. S., & Schiel, D. R. (2008). A dynamic energy budget model: parameterisation and application to the Pacific oyster *Crassostrea gigas* in New Zealand waters. *Journal of Experimental Marine Biology and Ecology*, *361*(1), 42-48.

Ren, J. S., Ross, A. H., & Schiel, D. R. (2000). Functional descriptions of feeding and energetics of the Pacific oyster *Crassostrea gigas* in New Zealand. *Marine Ecology Progress Series*, *208*, 119-130.

Reynolds C.S. (2006). The Ecology of Phytoplankton. Ecology, Biodiversity and Conservation. Cambridge University Press. 437 pp.

Rico-Villa, B., Bernard, I., Robert, R., & Pouvreau, S. (2010). A Dynamic Energy Budget (DEB) growth model for Pacific oyster larvae, *Crassostrea gigas*. *Aquaculture*, *305*(1), 84-94. doi: 10.1016/j.aquaculture.2010.04.018.

Rose, J. M., Bricker, S. B., Tedesco, M. A., & Wikfors, G. H. (2014). A role for shellfish aquaculture in coastal nitrogen management. *Environmental Science & Technology*, 48(5), 2519-2525. doi: 10.1021/es4041336

Ruesink, J. L., Lenihan, H. S., Trimble, A. C., Heiman, K. W., Micheli, F., Byers, J. E., & Kay, M. C. (2005). Introduction of non-native oysters: ecosystem effects and restoration implications. *Annual review of ecology, evolution, and systematics*, *36*, 643-689.

Sakshaug, E., & Holm-Hansen, O. (1977). Chemical composition of *Skeletonema costatum* (Grev.) Cleve and Pavlova (*Monochrysis*) *lutheri* (Droop) Green as a function of nitrate-, phosphate-, and iron-limited growth. Journal of Experimental Marine Biology and Ecology, 29(1), 1-34.

Samir, K. C., & Lutz, W. (2017). The human core of the shared socioeconomic pathways: Population scenarios by age, sex and level of education for all countries to 2100. *Global Environmental Change*, *42*, 181-192.

Slobodkin, L. B., & Richman, S. (1961). Calories/gm. in species of animals. *Nature*, *191*(4785), 299-299.

Suthers, I. M., & Rissik, D. (Eds.). (2009). *Plankton: A guide to their ecology and monitoring for water quality*. CSIRO publishing. Melbourne, Australia.

Tamayo, D., Ibarrola, I., Urrutxurtu, I., & Navarro, E. (2014). Physiological basis of extreme growth rate differences in the spat of oyster (*Crassostrea gigas*). *Marine biology*, *161*(7), 1627-1637.

Tetrault K. (2012). Reference Manual for SPAT Oyster Gardeners. SPAT - Southold Project in Aquaculture Training. Cornell Cooperative Extension of Suffolk Marine Program. 75 pp. Available at:
https://s3.amazonaws.com/assets.cce.cornell.edu/attachments/9506/SPAT_Manual.pdf?1435065245

van der Meer, J. (2006). An introduction to Dynamic Energy Budget (DEB) models with special emphasis on parameter estimation. *Journal of Sea Research*, *56*(2), 85-102.

Van Leeuwe, M., & De Baar, H. (2000). Photoacclimation by the Antarctic flagellate *Pyramimonas sp.(Prasinophyceae*) in response to iron limitation. European Journal of Phycology, 35(3), 295-303.

Velasco, L. A., & Navarro, J. M. (2002). Feeding physiology of infaunal (*Mulinia edulis*) and epifaunal (*Mytilus chilensis*) bivalves under a wide range of concentrations and qualities of seston. *Marine Ecology Progress Series*, *240*, 143-155.

Wallace, R. K., Waters, P., & Rikard, F. S. (2008). *Oyster hatchery techniques*. Southern Regional Aquaculture Center. Available at: http://fisheries.tamu.edu/files/2013/09/SRAC-Publication-No.-4302-Oyster-Hatchery-Techniques.pdf

Walne, P. R. (1972). The influence of current speed, body size and water temperature on the filtration rate of five species of bivalves. *Journal of the Marine Biological Association of the United Kingdom*, *52*(2), 345-374.

Walne, P. R., & Millican, P. F. (1978). The condition index and organic content of small oyster spat. *ICES Journal of Marine Science*, *38*(2), 230-233.

Ward, J.E. & S.E. Shumway. 2004. Separating the grain from the chaff: particle selection in suspension- and deposit-feeding bivalves. Journal of Experimental Marine Biology and Ecology 300: 83-130. doi:10.1016/j.jembe.2004.03.002

Weber, K., Hoover, E., Sturmer, L., & Baker, S. (2008). The Role of Dissolved Oxygen in Hard Clam Aquaculture.

Willmott, C. J., Ackleson, S. G., Davis, R. E., Feddema, J. J., Klink, K. M., Legates, D. R., ... & Rowe, C. M. (1985). Statistics for the evaluation and comparison of models. *Journal of Geophysical Research: Oceans*, *90*(C5), 8995-9005.

Winberg, G. G. (1960). Rate of metabolism and food requirements of fishes. *Fish. Res. Bd Can., Trans. Ser.*, *194*, 1-202.

Winter, J. E. (1978). A review on the knowledge of suspension-feeding in lamellibranchiate bivalves, with special reference to artificial aquaculture systems. *Aquaculture*, *13*(1), 1-33.

Worm, B., Barbier, E. B., Beaumont, N., Duffy, J. E., Folke, C., Halpern, B. S., ... & Sala, E. (2006). Impacts of biodiversity loss on ocean ecosystem services. *science*, *314*(5800), 787-790.

Zhou, S., Smith, A. D., & Knudsen, E. E. (2015). Ending overfishing while catching more fish. *Fish and Fisheries*, *16*(4), 716-722.